Polarforschung 79 (2), 81 – 96, 2009 (erschienen 2010)

Re-Coring at Ice Island T3 Site of Key Core FL-224 (Nautilus Basin, Amerasian Arctic): Sediment Characteristics and Stratigraphic Framework

by Ruediger Stein[1], Jens Matthiessen[1] and Frank Niessen[1]

Abstract: As shown in numerous studies of sediment cores from the Amerasian Basin, the lithostratigraphy of CLARK et al. (1980) seems to be a very useful tool for core correlation and for getting a relative stratigraphic framework in large parts of the Amerasian Basin. Because from Clark's cores collected from Ice Island T3 in the Amerasian Basin between 1952 and 1974, neither untouched archive and fresh (unaltered) sediment material nor state-of-the-art paleo-records used in modern paleoceanography (e.g., stable isotopes, geochemical proxies, MSCL logging, and XRF scanning), are available, a precise correlation to more recently recovered sediment cores from the Amerasian and Eurasian basins is difficult or even not possible. Thus, sediment core PS72/392-5 was recovered in the Nautilus Basin, a small sub-basin of the Canada Basin in the vicinity of the Mendeleev Ridge, during RV „Polarstern" ARK-XXIII/3 expedition in 2008 at the same location as Clark's key core FL-224. In core PS72/392-5, all the thirteen standard lithostratigraphic (SL) units A through M developed by CLARK et al. (1980), including the most prominent pink-white/white layers PW1, PW2 and W3, could clearly be identified. Future studies of this unique core material will allow to use up-to-date tools and methods in paleoceanography needed for a precise core correlation, a development of a more accurate age model, and a more detailed reconstruction of the circum-Arctic environmental history.
Based on a still preliminary age model, the more sandy intervals of SL units L, J, H, F, and C are correlated with periods of a maximum ice-sheet extent and its subsequent disintegration (glacial/deglacial phases) during glacial Marine Isotope Stages (MIS) 6, 8, 10, 12, and 16. Except MIS 6, these intervals are characterized by increased dolomite contents indicating ice-rafted debris (IRD) input from the Laurentide Ice Sheet (LIS). The dolomite-rich pink-white layers PW1 and PW2 probably represent short-lived events of IRD input related to a collapse of the LIS during MIS 8 and MIS 5d. During MIS 16 – for the first time – the LIS may have been large enough to reach the shelf break and release major amounts of (dolomite-laden) icebergs into the ocean when the disintegration of the LIS started. This still speculative hypothesis, however, has to be approved by further more detailed studies.

Zusammenfassung: CLARK et al. (1980) haben nach sedimentologischen Untersuchungen von einigen hundert Sedimentkernen aus dem Amerasischen Becken ein lithostratigraphisches Modell aufgestellt, das auf dreizehn lithostratigraphischen Standardeinheiten (SL) A bis M und weiteren charakteristischen Leithorizonten („pink-white layers") beruht und seitdem erfolgreich für die Korrelation von Sedimentkernen aus dem Amerasischen Becken angewendet wird. Leider gibt es von diesen zwischen 1952 und 1974 von der Eisinsel T3 gewonnenen Kernen keine intakten Archivhälften und z.T. auch keine Datensätze von modernen paläoozeanographischen Proxys, die heute routinemäßig zur Kernkorrelation und für Rekonstruktionen von Paläoumweltbedingungen eingesetzt werden. Dadurch ist eine fundierte Kernkorrelation über den gesamten Arktischen Ozean und die Erstellung eines Altersmodells für Arktis-Kerne bisher sehr schwierig bzw. nur eingeschränkt möglich. Um diese Lücke zu schließen, wurde während der "Polarstern" ARK- XXIII/3-Expedition der Sedimentkern PS72/392-5 an der Lokation von Clark's Schlüsselkern FL-224 genommen. In Kern PS72/392-5 konnten alle dreizehn SL-Einheiten A bis M eindeutig identifiziert werden. Damit steht für zukünftige Untersuchungen ein Probenmaterial zur Verfügung, das es erlauben wird, mittels neuer sedimentologischer, geochemischer und mikropaläontologischer Proxys sowie MSCL-Logging und XRF-Scanning-Daten Sedimentkerne vom Amerasischen und Eurasischen Becken eindeutiger zu korrelieren und besser stratigraphisch bzw. altersmäßig einzustufen.
Einige der SL-Einheiten in Kern PS72/392-5, die Einheiten L, J, H, F und C, zeichnen sich durch hohe Gehalte an Grobfraktion aus, die auf Transport durch Eisberge zurückgeführt werden. Der hohe Dolomit-Gehalt der Grobfraktion (mit Ausnahme der SL-Einheit L) weist auf den Kanadischen Archipel als Liefergebiet hin und wird mit dem Zerfall eines ausgedehnten Laurentischen Eisschildes (LIS) am Ende der Glazialstadien 8, 10, 12 und 16 interpretiert. Um diese spekulative Hypothese zu belegen, sind jedoch weitere detaillierte Untersuchungen erforderlich.

INTRODUCTION AND BACKGROUND

For Arctic Ocean sediments, several problems such as poor preservation of calcareous and biosiliceous microfossils in Arctic cores, result in difficulties in establishing accurate age-depth relationships in the existing sediment cores (see BACKMAN et al. 2004 *cum lit.*). Despite significant progress during the last years, the precise stratigraphic correlation and dating of the existing sediment cores from the Amerasian and Eurasian basins, is still a major challenge in Arctic paleoceanographic research (JAKOBSSON et al. 2000, BACKMAN et al. 2004, 2009, POLYAK et al. 2004, 2009, SPIELHAGEN et al. 2004, KAUFMAN et al. 2008, SELLÉN et al. 2008).

For the Amerasian Basin, a widely applied standard lithostratigraphy was developed by CLARK et al. (1980), which has provided a common stratigraphic framework for many investigators to correlate sediments across large areas of the Arctic Ocean. This framework is based on a detailed sedimentological study of several hundreds of short sediments cores collected from Ice Island T3 in the Amerasian Basin between 1952 and 1974 (Fig. 1A). In their study, CLARK et al. (1980) established 13 standard lithostratigraphic (SL) units A to M, which include silty and arenaceous lutites, and carbonate-rich, pinkish-white layers, with variable characteristic contents of quartz-feldspar, detrital grains (carbonate maxima; DARBY 1975), foraminifers, and Fe-Mn particles (Fig. 2). The content of sand-sized material (enriched in SL units C, F, H, J, L, and parts of M) and the pink-white layers were considered to be the key sedimentary characteristic used for correlation of these lithostratigraphic units. In the CESAR (Canadian Expedition to Study the Alpha Ridge) cores recovered from a drifting ice camp in 1983 (JACKSON et al. 1985), SL units A to M were also identified, and the lithostratigraphic successsion was even expanded by three new lithostratigraphic units A1, A2, and A3 recovered in CESAR core 83-14 (MUDIE & BLASCO 1985; for critical discussion see CLARK et al. 1990; for location of core see Fig. 1C).

[1] Alfred Wegener Institute for Polar and Marine Research AWI, Am Alten Hafen, 27568 Bremerhaven, Germany.

Manuscript received 10 August 2009, accepted in revised form 28 September 2009)

To obtain a chronological framework, Clark's lithostratigraphic units were correlated to paleomagnetic records determined in these cores. This first chronology of sediment cores from the Amerasian Basin was based on the assumption that zones with negative inclination represented genuine polarity reversals (STEUERWALD et al. 1968, CLARK et al. 1980, MINICUCCI & CLARK 1983). At that time, geomagnetic excursions have not been considered as an alternative to polarity reversals when interpreting paleomagnetic data in sediment cores. Thus, the first encountered down-core zone with negative inclination was interpreted to be the Brunhes/Matuyama boundary, occurring within SL Unit K. Later, the original age model was revised several times (BACKMAN et al. 2004 *cum lit.*). As shown in several studies during the last decade, a large number of measured changes in Pleistocene magnetic polarity directions in Arctic Ocean sediments probably represent rather geomagnetic excursions of shorter durations within the Brunhes Chron than full geomagnetic reversals (JAKOBSSON et al. 2001, NOWACZYK et al. 2001, 2003, SPIELHAGEN et al. 2004, KAUFMAN et al. 2008). For the Lomonosov Ridge area, a detailed late Pleistocene stratigraphy has been developed at core 96/12-1pc (Fig. 1C) using sediment physical properties including colour, paleomagnetism, biostratigraphy, chemostratigraphy, and optically stimulated luminescence dating (JAKOBSSON et al. 2000, 2001, 2003). In this core, distinct (cyclic) alternations of (dark) brown and beige to gray lithological intervals are described, with brown beds probably representing interglacial/interstadial periods and beige to gray beds corresponding to glacial/deglacial periods (see also PHILLIPS & GRANTZ 2001, POLYAK et al. 2004). Based on this revised chronostratigraphy, which is now widely accepted, the first major down-core polarity change (originally interpreted as Brunhes/Matuyama boundary) probably occurred within MIS 7 and correlates with the Biwa II or Pringle Falls excursion near 220-240 ka (BACKMAN et al. 2004, POLYAK et al. 2004, SPIELHAGEN et al. 2004, LUND et al. 2006, STEIN 2008). Very recently, however, it has been shown that paleomagnetic data determined in sedimentary sequences from the study area may be effected by post-depositional (diagenetic) processes (CHANNELL & XUAN 2009), making interpretation of paleomagnetic records again more difficult.

The lithostratigraphy approach of CLARK et al. (1980) seems to be a useful tool for core correlation and to establish a relative stratigraphic framework in large parts of the Amerasian Basin. Because from Ice Island T3 sediment cores studied by CLARK et al. (1980) neither untouched archive and fresh (unaltered) sediment material nor standard paleo-records used in

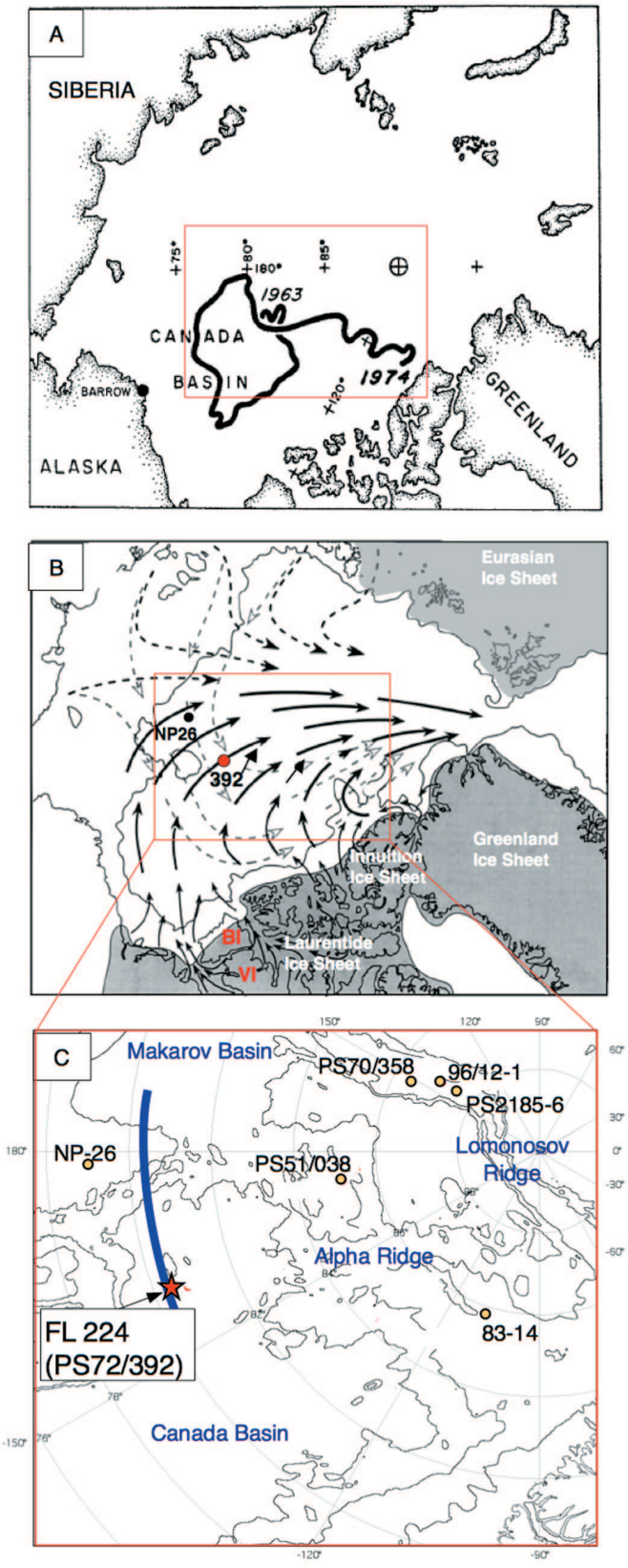

Fig. 1: (A) Track of ice island T-3 drift 1963-1974). All sediment cores studied by CLARK et al. (1980) were taken along this drift track (CLARK et al. 1980, supplemented). Red rectangle indicates area shown in (C).
(B) Map of the inferred current-driven iceberg drift directions from North American sources (solid arrows) and concurrent hypothesized drift of Siberian pack ice (broken arrows) during glacial intervals (BISCHOF & DARBY 1997, supplemented). As proposed by these authors, sea-ice drift in the western Arctic Ocean was mostly similar to the iceberg drift, but sea ice occasionally drifted from Siberian sources into the western Arctic Ocean along paths shown as broken arrows. The extension of late Quaternary (LGM) North American (i.e., Laurentide and Innutian), Greenland, and Eurasian ice sheets are indicated. Banks Island (BI) and Victoria Island (VI), potential source areas of the detrital-carbonate-rich pink-white layers, and locations of sediment cores NP-26 and PS72/392 are shown. Red rectangle indicates area shown in (C).
(C) Location map of cores discussed in the text. Blue line marks the location of the sampling transect across Mendeleev Ridge shown in Figure 3.

Abb.1: (A) Drift-Route der Eisinsel T3 in den Jahren 1963-1974. Alle von Clark und Mitarbeitern untersuchten Sedimentkerne wurden entlang dieser Route gewonnen (ergänzt nach CLARK et al. 1980).
(B) Karte der angenommenen Drift-Routen von Eisbergen mit nordamerikanischer Herkunft (durchgezogene Pfeile) und mit sibirischer Herkunft (gestrichelte Pfeile) während des letzten glazialen Maximums (ergänzt nach BISCHOF & DARBY 1997). Graues Raster = Ausdehnung der Eisschilde in Eurasien, Nordamerika und Grönland; BI = Banks Island, VI = Viktoria Island als potentielle Liefergebiete der Dolomit-reichen „pink-white layers"; Kern-Lokationen NP-26 und PS72/392 sind dargestellt.
(C) Karte der Positionen der im Text diskutierten Sedimentkerne.

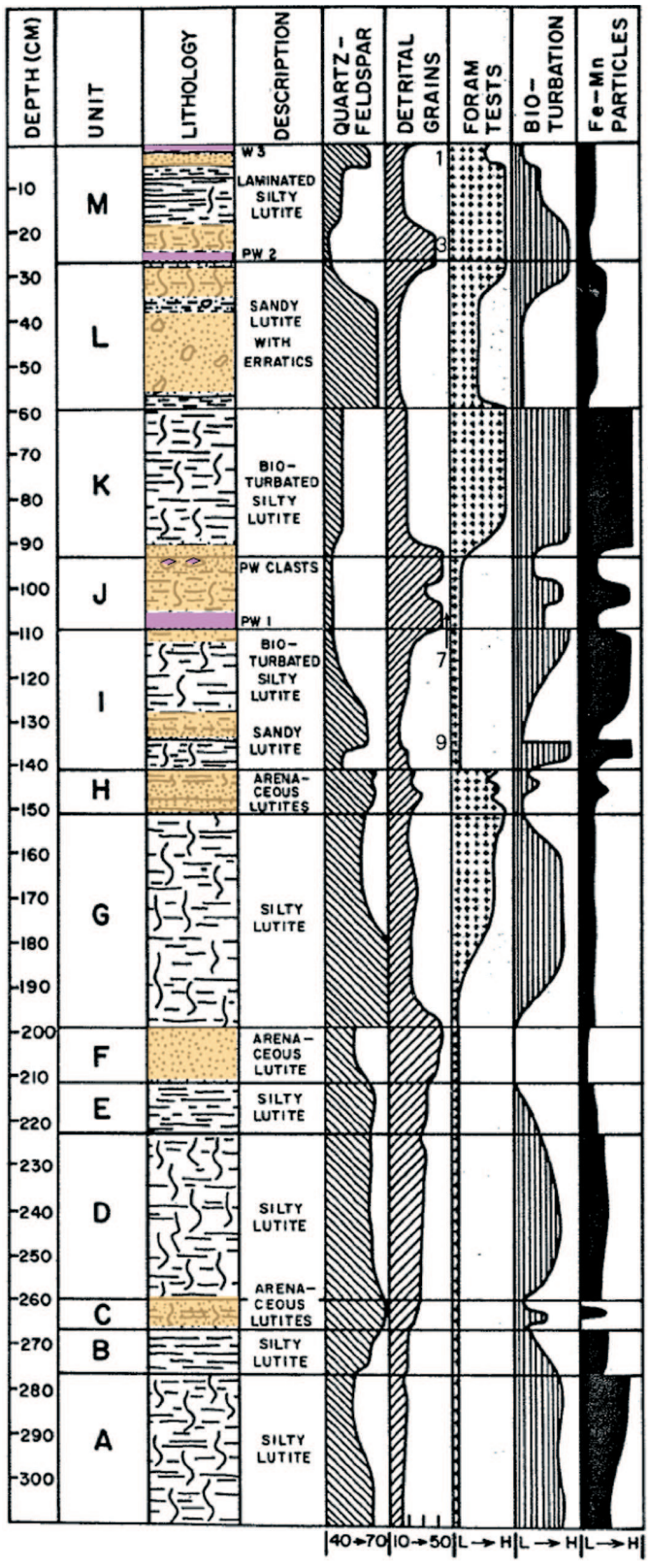

Fig. 2: Standard lithostratigraphy of the Alpha Ridge area (Amerasian Basin) based on a detailed sedimentological study of several hundreds of short sediment cores collected from Ice Island T3 (CLARK et al. 1980). In this stratigraphic framework, 13 standard lithostratigraphic (SL) units A to M were identified. Sedimentary parameters shown are percentages of quartz-feldspar, total detrital grains, foraminifer tests, level of bioturbation, and Fe-Mn particles. pw = pink white layer; w = white layer.

Abb. 2: Standard-Lithostratigraphie für das Gebiet des Alpha-Rückens, basierend auf sedimentologischer Untersuchung einiger hundert Sedimentkerne, die von der Eisinsel T3 gewonnen wurden (CLARK et al. 1980). In diesem lithostratigraphischen Schema wurden 13 lithostratigraphische (SL) Einheiten A bis M identifiziert. Die gezeigten Parameter umfassen relative Angaben zum Gehalt von Quarz und Feldspat, Anzahl der detritischen Körner, Foraminiferen-Schalen, Grad der Bioturbation und Vorkommen von Fe-Mn-Partikeln.

modern paleoceanography, are available, a precise correlation of these cores to more recently recovered and studied sediment cores from the Amerasian and Eurasian basins is difficult or even not possible as recently outlined by SELLÉN et al. (2008). According to these authors, for example,
(i) an exact colour correlation is not possible due to the lack of core photos of the T3 cores;
(ii) only interpreted zones of paleomagnetic polarity directions are available, but no paleomagnetic basis data including paleointensity values; and
(iii) coarse-fraction contents are only available based on few average values but no detailed records of discrete samples in T3 cores.

Having these difficulties in mind, core PS72/392-5 was recovered during RV "Polarstern" ARK-XXIII/3 expedition in the Nautilus Basin, a small sub-basin of the Canada Basin in the vicinity of the Mendeleev Ridge, at the same location as Clark's core FL-224 (Fig. 3; see cruise report JOKAT 2009; STEIN et al. 2009b). Core FL-224 was one of the reference cores for magnetostratigraphy (STEUERWALD et al. 1968; later revised by CLARK et al. 1980) and lithostratigraphy, making this core a key core for the lithostratigraphic and chronologic framework of the Amerasian Basin. Whereas the lowermost part of core FL-224 is disturbed by flow-in structures (CLARK et al. 1980) the new core PS72/392-5 (Fig. 3) does not show any coring disturbances throughout. Thus, re-coring at the location of core FL-224 will allow to re-study the sediment sequence of the „old" core in great detail, using well established standard methods, such as photography, visual core description, coarse fraction analysis, stable oxygen and carbon isotopes on foraminifers, state-of-the-art paleomagnetic data including paleointensity, but also new tools such as core logging, colour and XRF scanning. This will give the unique possibility for more precise correlation of the T3 sediment cores with more recently taken cores from the Amerasian and Eurasian basins, and, thus, the development of a more precise stratigraphic framework throughout the entire central Arctic Ocean.

MATERIAL AND METHODS

Core PS72/392-5 with a recovery of 6.15 m was obtained during RV "Polarstern" ARK-XXIII/3 expedition in 2008 at 80°27.81' N, 158°49.75' W in a water depth of 3624 m (Fig. 3, Tab. 1; JOKAT 2009) at the location of core FL-224 (CLARK et al. 1980). The water depth of core FL-224 seems to be about 150 m shallower than core PS72/392-5 (Tab. 1). This may be explained by a more „up-slope" location and/or less accurate determination of water depth and location at times when Core FL-224 was taken.

For sampling the sediment surface and undisturbed near-surface sediments, a giant box core (GKG) was also taken at the same station (PS72/392-6; Tab. 1). Furthermore, a second

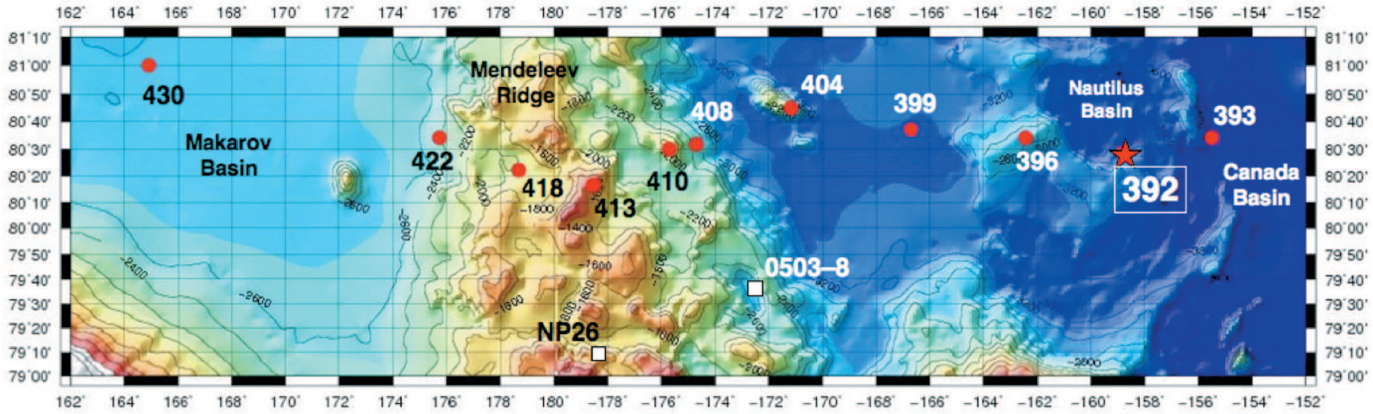

Fig. 3: Locations of geological stations carried-out at the northern transect across Mendeleev Ridge during "Polarstern"AKR-XXIII/3 expedition. (392 = PS72/392; 393 = PS72/393, etc.). In addition, locations of cores NP-26 and 0503-8 (= HLY0503-8JPC) are shown.

Abb.3: Positionen der geologischen Stationen, die auf dem nördlichen Transekt über den Mendeleev-Rücken während der Expedition AKR-XXIII/3 beprobt wurden (392 = PS72/392, 393 = PS72/393, etc.). Zusätzlich sind die Positionen der Kerne NP-26 und 0503-8 (= HLY0503-8JPC) gezeigt.

Station	Gear	Latitude	Longitude	WD (m)
PS72/392-4	GC	80° 28.31' N	158° 50.86' W	3632
PS72/392-5	GC	80° 27.81' N	158° 49.75' W	3624
PS72/392-6	GKG	80° 28.42' N	158° 50.83' W	3637
PS72/396-3	GKG	80° 35.17' N	162° 22.57' W	2733
PS72/396-5	KAL	80° 34.74' N	162° 19.01' W	2722
FL 224	GC	80° 27.74' N	158° 48.81' W	3467
PS2185-6	KAL	87° 32.20' N	144° 55.60' E	1052
PS70/358-4	KAL	86° 31.57' N	152° 09.63' E	1464

Tab. 1: Locations and water depths of geological stations carried-out during „Polarstern"ARK-XXIII/3 expedition in 2008 and discussed in this paper (for complete list of all geological stations see JOKAT 2009). WD = water depth; GC = Gravity Corer; GKG = Giant Box Corer; KAL = Kastenlot. In addition, data from core FL 224 (CLARK et al. 1980), PS2185-6 (FÜTTERER 1992), and PS70/358-4 (SCHAUER 2008) are listed.

Tab. 1: Lokationen und Wassertiefen ausgewählter geologischer Stationen der „Polarstern"-Expedition ARK-XXIII/3 (JOKAT 2009). Zusätzlich sind Daten der Kerne FL 224 (CLARK et al. 1980), PS2185-6 (FÜTTERER 1992) und PS70/358-4 (SCHAUER 2008) aufgelistet.

gravity core PS72/392-4 (Tab. 1) with a recovery of 5.68 m was recovered to double the amount of sediments available for later studies on this key core section.

Before opening, core PS72/392-5 was logged onboard RV "Polarstern" for measurement of magnetic susceptibility, density, and p-wave velocity using the Multi Sensor Core Logger (MSCL, GEOTEK Ltd., UK; WEBER et al. 1997).

After opening, from all core sections photographs were taken, and a detailed visual core description was carried out (Tab. 2). Colour of sediments was described using the Munsell Soil Colour Chart.

For main lithologies, smear-slide analyses were performed for rough evaluation of grain-size composition, preliminary determination of mineralogical composition (quartz, feldspars, carbonates, opaques), and content of biogenic components (foraminifers, coccoliths, diatoms, sponge spicules).

Spectral reflectance was measured on freshly split core surfaces using a Minolta CM 2002. In this paper, only the gray scale value L* is used (for more details see STEIN et al. 2009b).

X-Ray photographs were taken from sediment slabs of 25 cm x 10 cm x 0.8 cm each in order to count the numbers of coarse grains >2 mm which are mainly related to ice-rafted debris (IRD; Grobe 1987) and to study the sediment structures in detail (see MATTHIESSEN et al. 2010, this vol.).

Shore based investigations were carried out at the Alfred Wegener Institute (AWI). 190 samples from core PS72/392-5 were analysed for mineralogy and total organic carbon and carbonate contents (sampling space of 1-3 cm in the upper 260 cm and at 5 cm intervals below 260 cm).

In all samples, relative abundances of quartz, feldspars, dolomite, and calcite were estimated by X-ray diffraction (XRD) technique. For XRD measurements, a split of 1-2 g of ground bulk sediment was measured continuously using a Phillips PW3020 diffractometer equipped with cobalt kα radiation, automatic divergence slit, graphite monochromator, and automatic sample changer. For the purpose of this study, i.e., for getting a first-order estimate of relative abundances of major mineral components of the sediment, a spectrum from 20 to 40° 2Theta, which involves the major peaks of quartz (3.34 Å, 4.26 Å), K-feldspar (3.23 Å), plagioclase (3.19 Å), calcite (3.04 Å), and dolomite (2.89 Å), was measured. Single peak intensities, i.e., peak heights, were calculated by the Mac-Diff programme (PETSCHIK 2000, MOROS et al. 2004, STEIN et al. 2009a). Because the 3.34 Å peak may also belong to other minerals (e.g., illite), for further evaluation the quartz peak at 4.26 Å (generally about 35 % of the intensity of the most intense peak at 3.34 Å) was used.

The determination of total carbon (TC) and total organic carbon (TOC) as basic parameters was performed on all 190 samples by standard LECO technique. Routinely, carbonate content is calculated using the inorganic carbon proportion (IC = TC-TOC), multiplied by 8.333:

Carbonate content (%) = IC • 8.333

assuming that calcite is the predominant carbonate phase.

Based on the XRD data, however, we know that major proportion of the inorganic carbon is related to dolomite ((Ca, Mg)$(CO_3)_2$) and/or calcite ($CaCO_3$). Furthermore, we also controlled whether other carbonate minerals such as siderite (2.79 Å, $FeCO_3$) and rhodochrosite (2.84 Å, $MnCO_3$), are present in the samples. Especially rhodochrosite as mineral with pinkish-red colours was of interest as possible cause for the colour of the pink-white horizons (http://webmineral .com/data/Rhodochrosite.shtml).

Based on our „screening method", both minerals seem to be either absent or occur in only very minor amounts, as checked for samples with high amount of inorganic carbon. In the pink-white layer PW2, it seems to be that rhodochrosite was slightly enriched. The significance of increased input of (detrital) rhodochrosite as sediment-source indicator and possible mechanism causing the pink colour, has to be tested by further detailed mineralogical (XRD) studies.

In our screening approach for getting first-order information about the presence of detrital carbonate (dolomite), we simply divided the inorganic carbon into its calcite and dolomite proportions using the relative intensity (r.i.) values of the calcite (3.04 Å) and dolomite (2.89 Å) XRD peaks and assuming that calcite plus dolomite equals to the total carbonate content:

$$\text{Calcite (\%)} = \frac{\text{Calcite}_{\,3.04\,\text{Å r.i.}}}{(\text{Calcite}_{\,3.04\,\text{Å r.i.}} + \text{Dolomite}_{\,2.89\,\text{Å r.i.}})} \bullet \text{IC} \bullet 8.333$$

$$\text{Dolomite (\%)} = \frac{\text{Dolomite 2.89 Å r.i.}}{(\text{Calcite}_{\,3.04\,\text{Å r.i.}} + \text{Dolomite}_{\,2.89\,\text{Å r.i.}})} \bullet \text{IC} \bullet 7.67$$

We are aware about that for getting more detailed information about different carbonate mineral phases such as, for example, low and high magnesium calcites, which may help to identify specific Arctic source regions, more detailed XRD studies (e.g., more sophisticated sample preparation, use of standards, evaluation of multiple mineral peaks etc.) are needed (see Dalrymple & Maass 1987, Vogt 1997, 2009, Nørgaard-Pedersen et al. 2007).

SEDIMENT CHARACTERISTICS AND LITHOLOGIES

Main lithologies

The most prominent feature of the sediments of core PS72/392-5 is the alternation of dark-brown to brown and olive-brown to beige colours occurring throughout the entire core. Below 430 cm core depth, the dark-brown (to dark reddish-brown) colours become more abundant, below 546 cm even predominant, intercalated by (light) yellowish brown intervals between 455 and 505 cm core depth. In total, 52 dark brown intervals were counted in the upper 546 cm (B1 to B52; Fig. 4). Based on detailed visual core description (Tab. 2) and smear-slide analysis, the sediments are mainly silty clay and sand-bearing silty clay. The sandy to sand-bearing intervals are restricted to the upper part of the core and the basis for separating the sedimentary section into two lithological units, Unit I (0-259 cm) and Unit II (259-600 cm, core base). Within Unit I, the more sandy intervals occur between 249 and 255 cm, 202 and 224 cm, 157 and 168 cm, 114 and 129 cm, and 68 and 83 cm core depth, and in the upper 59 cm. Prominent light reddish brown ("pinkish") horizons were found at 127-129 cm and 57-59 cm core depth (Figs. 4, 5). In addition, intervals with pinkish lenses, spots and/or lenses occur at 220, 215, 210, 159, 117, 81, and 31 cm (Fig. 4). According to smear-slide analysis, foraminifers and coccoliths are only observed in the upper 180 cm.

The uppermost part of the sedimentary sequence represented by the giant boxcorer (GKG) core PS72/392-6, is characterized by two distinct dark gray silty clay layers at 37-38 cm and 25-26 cm, and a very pale brown („white" W3) layer at 13-14 cm (Fig. 5). These layers correspond to the dark grey layers at 26 and 13 cm and the white layer at 6.5-7.5 cm, respectively, in core PS72/392-5 (Tab. 2). The different depth intervals are explained by a 2-4 cm coring loss and sediment compaction (during the coring process) in core PS72/392-5 recovered by gravity corer.

XRD, carbonate, and total organic carbon data

Relative XRD intensities of quartz (4.26 Å), plagioclase (3.19 Å) and K-feldspar (3.23 Å), and dolomite (2.89 Å) were determined as proxy for detrital input from surrounding continents. The relative intensity of calcite (3.04 Å) may be controlled by both detrital (terrigenous) and biogenic (foraminifers and coccoliths) carbonate input.

In general, a prominent change in main mineralogy coincides with the boundary of lithological units I and II (Fig. 6). Whereas Unit II displays predominantly low quartz/feldspar (Qua/Fsp) and K-feldspar/plagioclase (Kfs/Plag) ratios of <0.7, the Qua/Fsp and Kfs/Plag ratios show distinct peak values within Unit I. The onset of carbonate sedimentation occurred at the Unit II/I boundary as indicated in the inorganic (carbonate) carbon record (Fig. 6). Dolomite is absent in Unit II and slightly increases at the Unit II/I boundary, followed by a major increase at about 224 cm core depth. Peak dolomite abundances were determined in the pink-white and white layers. Calcite starts to occur at 181 cm core depth, below that level calcite is more or less absent (Fig. 6).

Based on the XRD data, it becomes obvious that by far the predominant proportion of carbonate is detrital (terrigenous), i.e., dolomite, as reflected in the up to one order of magitude higher dolomite intensity values (Fig. 6). Dolomite contents are estimated to vary between 0 and >50 % (Fig. 7), whereas calcite contents vary between 0 and 10 % (Fig. 8). Absolute dolomite maxima of 47.3 %, 52.5 %, and 42.1 % coincide with the pink-white layers PW1, PW2, and W3, respectively (Fig. 7). Most of the dolomite maxima do not correlate with calcite maxima (Fig. 8).

In general, total organic carbon (TOC) values are low, ranging between 0.05 and 0.40 % (Fig. 6). The higher TOC values were determined at 228-200 cm (0.15-0.26 %), at 75-85 cm (0.21-0.28 %), and in the upper 26 cm (0.2-0.4 %). The absolute TOC maxima of 0.40 and 0.38 % coincide with the dark grey

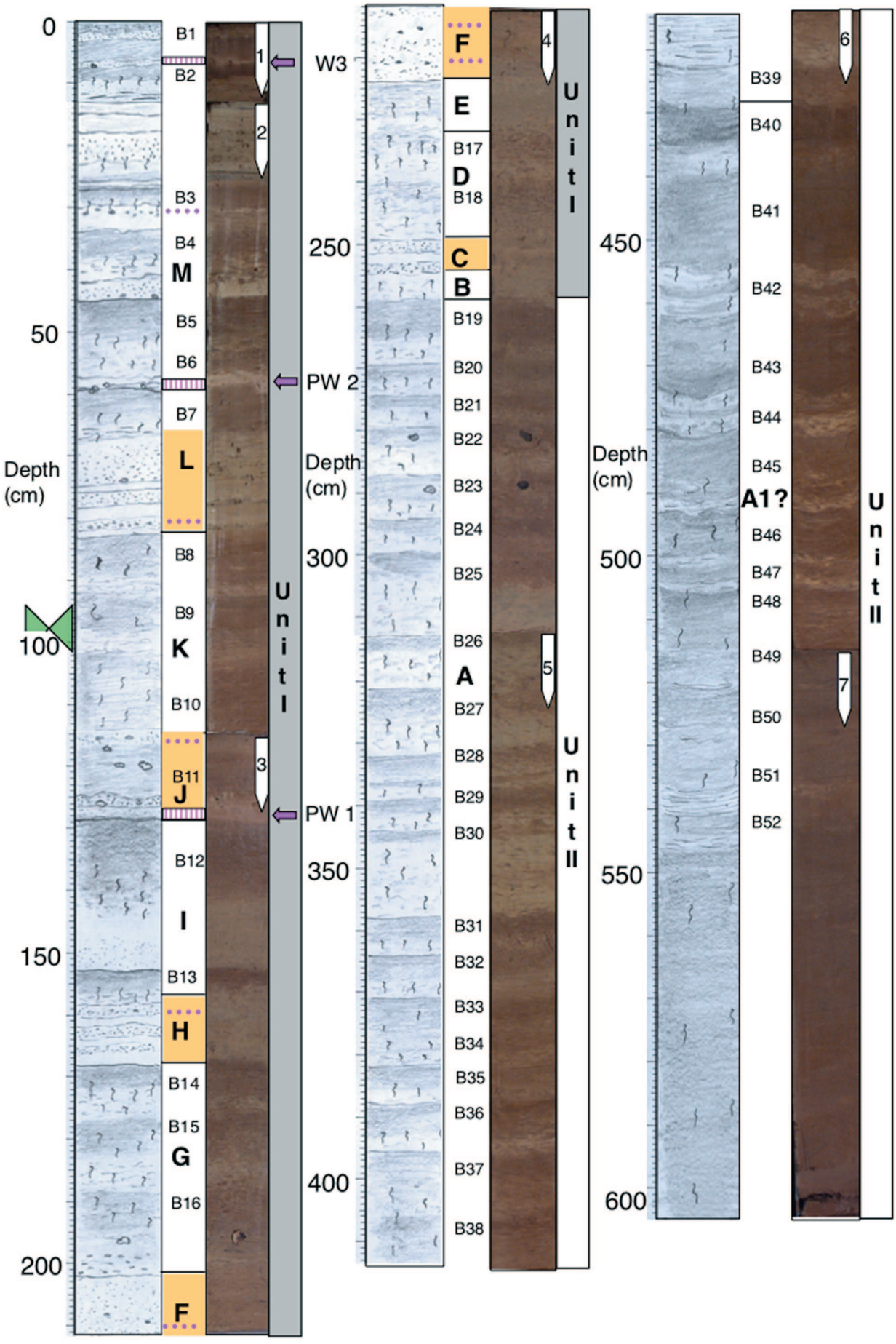

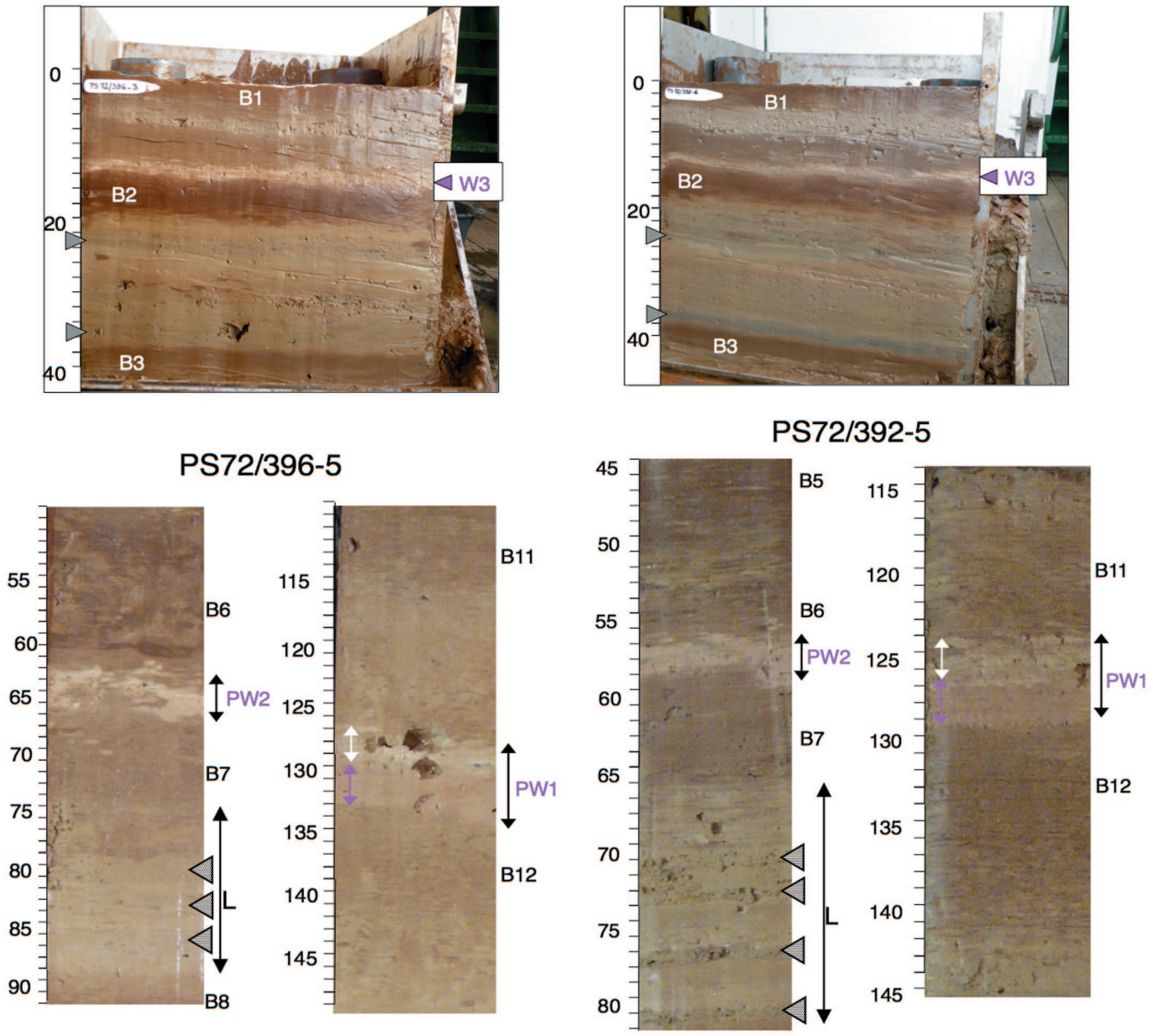

Fig. 5: Photographs of selected intervals from core loctions PS72/392 and PS72/396. Photographs of upper panels show giant box corers (GKG) PS72/392-6 and PS72/396-3, respectively, indicating the white layer (W3), dark-brown layers B1 and B2, and (marked by gray triangles) prominent gray layers. The lower panels from gravity cores PS72/392-5 and PS72/396-5 indicate the intervals around the pink-white layers PW2 and PW1. In the PW1 interval, an upper white layer and a lower pink layer can be separated. L marks SL Unit L with more sandy layers (gray triangles).

Abb. 5: Fotos ausgesuchter Intervalle der Kernlokationen PS72/392 und PS72/396. Die oberen Fotos sind von den Großkastengreifern PS72/392-6 und PS72/396-3 und zeigen die „white layer" W3 und die braunen Lagen B1 und B2 sowie markante graue Lagen. Die unteren Fotos sind von den Schwerelotkernen PS72/392-5 und PS72/396-5 und zeigen die Intervalle um die Lagen PW1 und PW2 („pink-white layer") und die Einheit L mit markanten Sandlagen (graue Dreiecke).

Fig. 4: Lithologies based on visual core description and core photographs of sections 1 to 7 of core PS72/392-5, which is a re-coring at the location of key core FL-224 of CLARK et al. (1980). All the 13 standard lithostratigraphic (SL) units A to M of CLARK et al. (1980) could clearly be identified. Below 430 cm core depth (i.e., the base of SL Unit A), another different lithological unit was separated, which may correlate with SL Unit A1 described by MUDIE & BLASCO (1985) in CESAR cores. Lower part of SL Unit L and SL units J, H, F, and C characterized by the occurrence of prominent more sandy intervals, are highlighted in yellow. Depths of white and pink-white layers (W3, PW2, and PW1) used for correlation (cf. CLARK et al. 1980), are marked. Pink-coloured dotted lines indicate occurrence of pinkish lenses/clasts. Dark-brown to brown intervals are counted down-core (B1 to B52). Main lithological Unit I (0-259 cm core depth, SL units M to B) and Unit II (259 to core base, SL units A and A1) are indicated. In core FL-224 (CLARK et al. 1980), the first major down-core magnetic polarity change was determined within SL Unit K at about 100 cm core depth, here marked as green triangle symbol in core PS72/392-5 at the same depth range (the exact depth level of this polarity change in the sequence of core PS72/392-5 still has to be determined in a future study). Depending on the age model, this polarity change has been correlated with the Brunhes/Matuyama boundary or Marine Isotope Stage 7 (CLARK et al. 1980, BACKMAN et al. 2004, STEIN 2008).

Abb.4: Lithologie und Kernfotographien der Sektionen 1 bis 7 von Kern PS72/392-5, der von derselben Position wie der Schlüsselkern FL-224 von CLARK et al. (1980) gewonnen wurde. Alle 13 lithostratigraphischen Einheiten – A bis M – konnten auch im Kern PS72/392-5 identifiziert werden. Der untere Teil von Einheit L and die Einheiten J, H, F und C, die durch deutlich erhöhte Sandgehalte gekennzeichnet sind, sind gelb markiert. Die Tiefen der Lagen W3 („white layer"), PW2 und PW1 („pink-white layer"), sowie das Vorkommen der pink-farbenen Linsen und Klasten (vgl. CLARK et al. 1980) sowie die braunen bzw. dunkelbraunen Lagen B1-B52 sind angezeigt. In Kern FL-224 ist innerhalb der Einheit K bei 100 cm Tiefe ein Wechsel der magnetischen Polarität gemessen worden, der – je nach Altersmodell – mit der Brunhes/Matuyama-Grenze bzw. dem Marinen Isotopen-Stadium 7 korreliert wird (CLARK et al. 1980, BACKMAN et al. 2004, STEIN 2008). Dieser Polaritätswechsel ist im Kern PS72/392-5 im entsprechenden Tiefenniveau durch das grüne Dreieckssymbol angedeutet.

SL unit (cm)	Depth (cm)	Lithology
	0 - 2	brown (10YR 4/3) (sandy) silty clay
	2 - 3	grayish brown (2.5Y 5/2) (sandy) silty clay; some gray mud clasts
	3 - 6.5	dark grayish brown (10YR 4/2) silty clay
	6.5 - 7.5	very pale brown (10YR 7/ 3) (sandy) silty clay; dropstone (0.5 cm in diameter) at 7.5 cm („white layer W3"; at 13-14 cm in GKG)
	7.5 - 10	dark brown (10YR 3/3) silty clay; at 9-10 cm yellowish brown mottling
	10 - 15	olive brown (2.5Y 4/3) (sandy) silty clay; some lamination, at 13 cm (25 cm in GKG) dark gray (2.5Y 4/1) horizon; 14.5-15 cm more fine-grained and lighter (2.5Y 5/3)
	15 - 18	yellowish brown (10YR 5/4) silty clay; very dark gray lamina at 16 cm
	18 - 23.5	olive brown (2.5Y 4/3) sandy silty clay
	23.5 - 25.5	olive gray (5Y 4/2) silty clay, some sand; some yellowish brown mottling
M	25,5 - 26.5	dark gray (2.5Y 4/1) silty clay; sharp contact at base (interval at 37-38 cm in GKG)
(59)	26.5 - 27	yellowish brown (10YR 5/6) silty clay; sharp contact at base
	27 - 30	dark brown (10YR 3/3) silty clay; gradational contact at base
	30 - 34	yellowish brown (10YR 5/4) and dark brown (10YR 3/3) (sandy) silty clay; some lamination; small very pale brown (10YR 7/3) and pinkish clasts; two dropstones (0.5 and 1 cm in diameter) at 31 cm
	34 - 39	dark brown (10YR 3/3) silty clay
	39 - 42	yellowish brown (10YR 5/4) and dark brown (10YR 3/3) silty clay; strongly motted (Planolites)
	42 - 45	light yellowish brown (2.5Y 6/3) (sandy) silty clay; some mud clasts; „white" lense on top, small dropstone (0.5 cm in diameter) at the base; very sharp contact at base
	45 - 57	dark brown (10YR 3/3) silty clay; yellowish brown to brown mottling, most significant in middle part and decreasing upward
	57 - 59	light yellowish brown (10YR 6/3) and light reddish brown (2.5YR 6/3) sandy silty clay; several dropstones of 0.5 to 1.5 cm in diameter („pink-white layer PW2")
L	59 - 68	brown (10YR 4/3) (sandy) silty clay, fining upward; gradational contact at base
(24)	68 - 83	light olive brown (2.5Y 5/3) to olive brown (2.5Y 4/3) sandy silty clay, abundant olive and (some) pinkish – especially at 81-82 cm – dark gray clasts; silty clay intervals at 75-76, 78.5-81, and 82-83 cm
K (31)	83 - 114:	brown (10YR 4/3) to dark brown (10YR 3/3) silty clay; bioturbated, light olive brown mottling, especially at 91-92 and 100-103; some lamination
	114 - 124	brown (10YR 4/3) and yellowish brown (10YR 5/4) silty clay (some sand in uppermost part); dropstones (0.5-1 cm in diameter) at 117 and 121 cm; some pinkish lenses/clasts at 117 cm; some small Fe-Mn micronodules
J (15)	124 - 127	light yellowish brown (10YR 6/4) and brown (10YR 4/3) sandy silty clay; small light yellowish brown clasts; dropstones at 125 cm (0.5 cm in diameter) and 126 cm (1 cm in diameter)
	127 - 129	light reddish brown (2.5YR 6/3) (sandy) silty clay („pink-white layer PW1"); sharp contact at base
	129 - 142	brown (10YR 4/3) silty clay; dark brown and light olive brown mottling; Fe-Mn micronodules in upper part
I	142 - 153	light olive brown (2.5Y 5/3) and olive gray (5Y 5/2) sandy silty clay; fining upward; sharp contact at base
(28)	153 - 157	brown (10YR 4/3) silty clay; lower half strongly mottled (light olive brown 2.5Y 5/3); Fe-Mn micronodules in upper brown part
H (11)	157 - 168	light olive brown (2.5Y 5/4) and yellowish brown (10YR 5/4) sandy silty clay (157-160, 162-164, and 165-168 cm) to silty clay (160-162 and 164-165 cm); olive gray spots/lenses at 164-168 cm, pinkish lenses at 159 cm; sharp contact at base
	168 - 196	alternation of brown (10YR 4/3) (168-173, 177-184, and 188-196 cm) and light olive brown (2.5Y 5/3) (173-177 and 184-188 cm) silty clay; strong dark brown and yellowish brown mottling (strongly bioturbated; Chondrites-type); abundant small Fe-Mn micronodules at 169-181 and 188-193 cm
G (34)	196 - 202	light olive brown (2.5Y 5/3) (sandy) silty clay, abundant dark gray/dark olive gray lenses/clasts; dropstone (2 cm in diameter) at top
F (22)	202 - 224:	yellowish brown (10YR 5/4) sandy silty clay, more sandy in lower part (fining upward); some dark graay, dark olive gray, and pinkish lenses/clasts; several small dropstones (< 0.4 cm) at 208, 209, 213, 215, 216, 221, and 222 cm; Fe-Mn micronodules; sharp contact at base
E (7)	224 - 231	light olive brown (2.5Y 5/3) and olive gray (5Y 5/2) silty clay; some mottling/bioturbation; gradational contact at base
D (18)	231 - 249	dark brown (10YR 4/3) and light olive brown (2.5Y 5/4) silty clay; strongly bioturbated (Chondrites-type)
C (6)	249 - 255	yellowish brown (10YR 5/4) and light olive brown (2.5Y 5/4) sandy silty clay (249-251 and 252-255 cm) and silty clay (251-252 cm); Fe-Mn micronodules
B (4)	255 - 259	light olive brown (2.5Y 5/3) silty clay; some dark brown mottling; Fe-Mn micronodules

Tab. 2: Detailed lithological core description of gravity core PS72/392-5 – recovered at the same location as core FL-224 – carried-out onboard "Polarstern". "Standard Lithostratigraphic (SL) units" are classified as A1 to M, following CLARK et al. (1980) and MUDIE & BLASCO (1985). In brackets below thickness of SL units in cm are given.

Tab. 2: Detaillierte lithologische Kernbeschreibung von Sedimentkern PS72/392-5. Standard-lithostratigraphische (SL) Einheiten nach CLARK et al. (1980) und MUDIE & BLASCO (1985). Mächtigkeiten der SL-Einheiten in cm in Klammern.

Table 2 continued		
	259 - 305	alternation of dominantly brown (10YR 4/3) and more light olive brown (2.5Y 5/4) silty clay (brown intervals at 259-266, 269-272,274-277, 279-283, 287-292, 294-297, and 300-304 cm); strongly mottled/bioturbated (Chondrites-type); Fe-Mn-coated dropstones (1-2 cm in diameter) at 281 and 289 cm; Fe-Mn micronodules; gradational contact at base
	305 - 313	light olive brown (2.5Y 5/Table continued4) and olive gray (5Y 5/2) silty clay, some sand; strongly mottled; Fe-Mn micronodules
	313 - 414	alternation of brown (10YR 4/3) (to dark brown 10YR 3/3) and light olive brown (2.5Y 5/4) silty clay (brown at 313-315, 321-327, 332-335, 336-337, 339-342, 344-346, 358-362, 364-368, 371-380, 382-386, 387-393, 399-414 cm; dark brown at 287-390, 396-399, and 405-408 cm; light olive brown in between); dark brown
A (171)	414 - 416	mottling/strongly bioturbated; Fe-Mn micronodules (more abundant above 367 cm)
	416 - 424	brown (10YR 5/3) silty clay
	424 - 430	brown (10YR 4/3) and yellowish brown (10YR 5/4) silty clay; at 421-423 cm also pale yellow (2.5Y 7/4) colours; some lamination (check X-Ray) and mottling/ bioturbation; some Fe-Mn micronodules
		brown (10YR 4/3 to 5/3) silty clay; some mottling/bioturbation; some Fe-Mn micronodules
A1? (>185)	430 - 437	dark reddish brown (5YR 3/2) silty clay
	437 - 455	dark brown (10YR 3/3) to dark reddish brown (5YR 3/2) silty clay; some thin brown (lighter) laminae at 437-439 cm
	455 - 463	yellowish brown (10YR 5/4) and dark brown (10YR 3/3) silty clay; moderately mottled/bioturbated; dark brown at 457-459 cm
	463 - 477	dark brown (10YR 3/3) silty clay; slightly mottled/bioturbated
	477 - 515	dark brown (10YR 3/3) to brown (10YR 4/3) silty clay with intervals of light yellowish brown (10YR 6/4) and yellowish brown (10YR 5/4) laminae/spots (most prominent at 478-481, 488-489, 491-493, 499-500, and 503-504 cm); some bioturbation/mottling; Fe-Mn micronodules throughout
	515 - 615	dark brown (10YR 3/3) silty clay, slightly mottled (brown); at 521 cm thin light yellowish brown (10YR 6/4) lamina; at 537-541 and 544-546 cm light yellowish brown laminae/spots; Fe-Mn micronodules at 515-522 cm

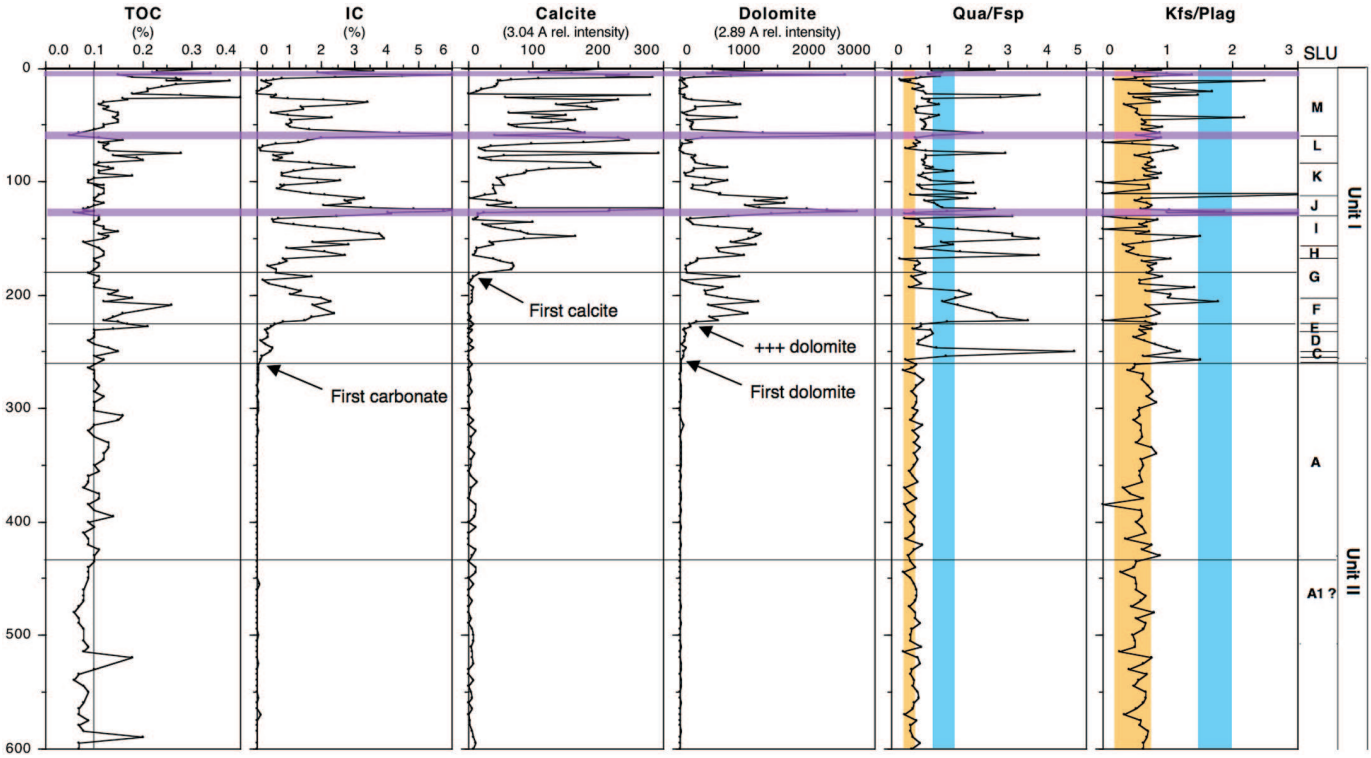

Fig. 6: Total organic carbon (TOC), inorganic carbon (IC), relative XRD intensities of calcite (3.04 Å) and dolomite (2.89 Å), and quartz/feldspar and K-feldspar/plagioclase intensity ratios in samples from core PS72/392-5 (For feldspar intensity, relative intensities of the plagioclase and K-feldspar peaks were added). Standard lithostratigraphic (SL) units A1 to M ("SLU") according to CLARK et al. (1980), main lithological units (Unit I and Unit II, and depths of main pink-white layers are indicated. The pink-white layers are characterized by absolute dolomite peak intensity maxima. Orange bars and blue bars indicate range of typical quartz/feldspar and K-feldspar/plagioclase ratios determined in surface sediments from the Laptev Sea and Canadian Archipelago/Sverdrup Basin areas, respectively (according to VOGT 1997). Depths of onset of inorganic carbon and of dolomite (base of SL Unit C) and calcite (middle part of SL Unit G) and depth of major increase in dolomite (base of SL Unit F) are indicated. The inorganic (carbonate) carbon (%) values are in the same range as the low-resolution carbonate values determined at core FL-224 (DARBY et al. 1989).

Abb.6: Organischer (TOC) und anorganischer (IC) Kohlenstoffgehalt, relative XRD-Intensitäten von Kalzit (3.04 Å) und Dolomit (2.89 Å), und Quarz/Feldspat- and K-Feldspat/Plagioklas-Intensitätsverhältnisse in Proben von Kern PS72/392-5. Standard-lithostratigraphische (SL) Einheiten A1 bis M („SLU") nach CLARK et al. (1980), Haupt-lithologische Sediment-Einheiten I und II und Tiefen der Lagen W3, PW2 und PW1, die durch absolute Maxima in den Dolomitgehalten charakterisiert werden, sind angezeigt. Orange und blaue Balken zeigen den Bereich typischer Quarz/Feldspat- and K-Feldspat/Plagioklas-Intensitätsverhältnisse in Oberflächensedimenten aus dem Laptew-Meer bzw. der Region vom Kanadischen Archipel/Sverdrup-Becken (nach VOGT 1997). Die Gehalte an anorganischem (Karbonat) Kohlenstoff von Kern PS72/392-5 entprechen den von DARBY et al. (1989) in Kern FL-224 bestimmten Karbonatwerten.

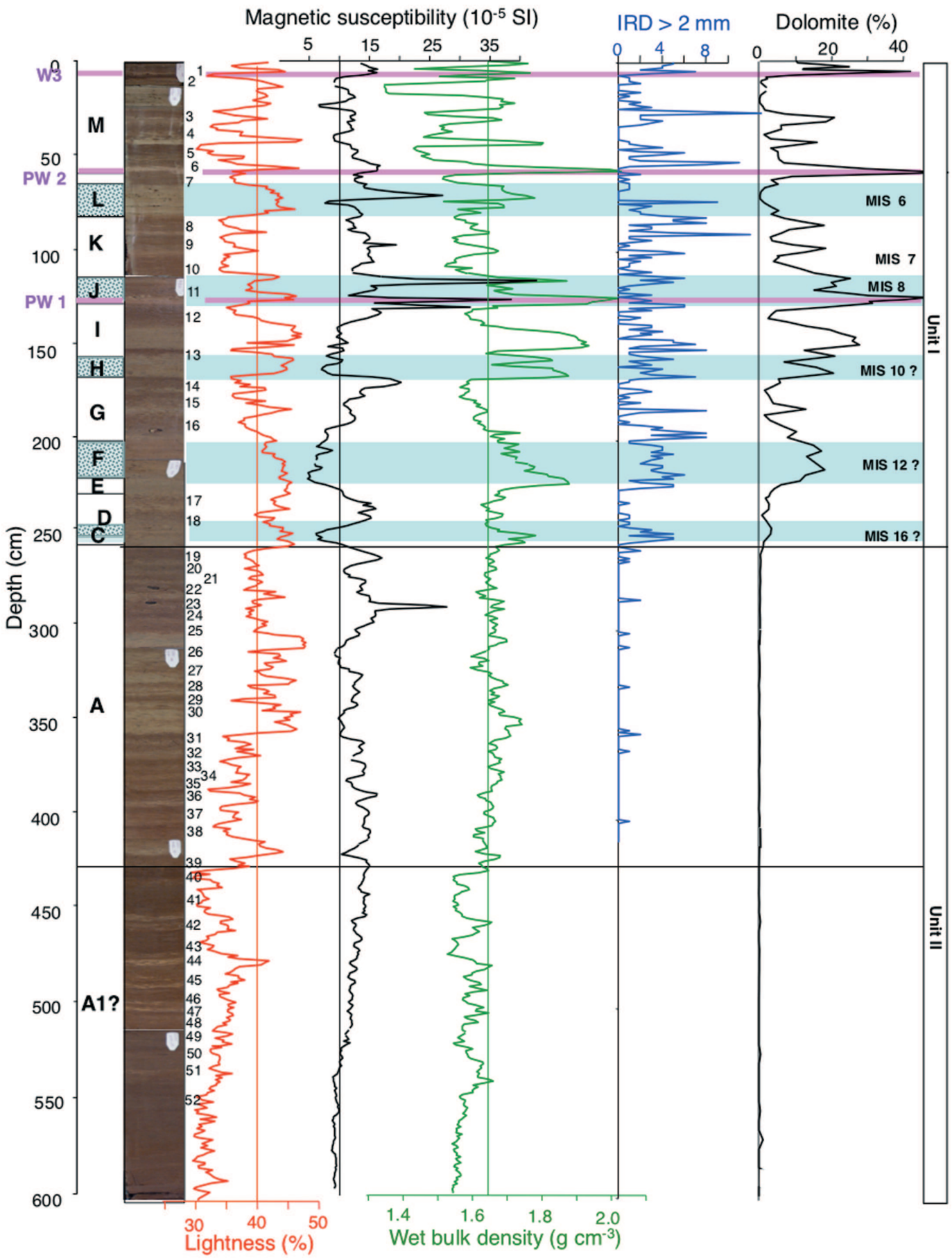
Magnetic susceptibility (10-5 SI)
5
15
25
35
IRD > 2 mm
0
4
8
Dolomite (%)
0
20
40
W3
PW 2
PW 1
M
L
K
J
I
H
G
F
E
D
C
A
A1?
MIS 6
MIS 7
MIS 8
MIS 10 ?
MIS 12 ?
MIS 16 ?
Unit I
Unit II
Depth (cm)
0
50
100
150
200
250
300
350
400
450
500
550
600
30
40
50
Lightness (%)
1.4
1.6
1.8
2.0
Wet bulk density (g cm-3)

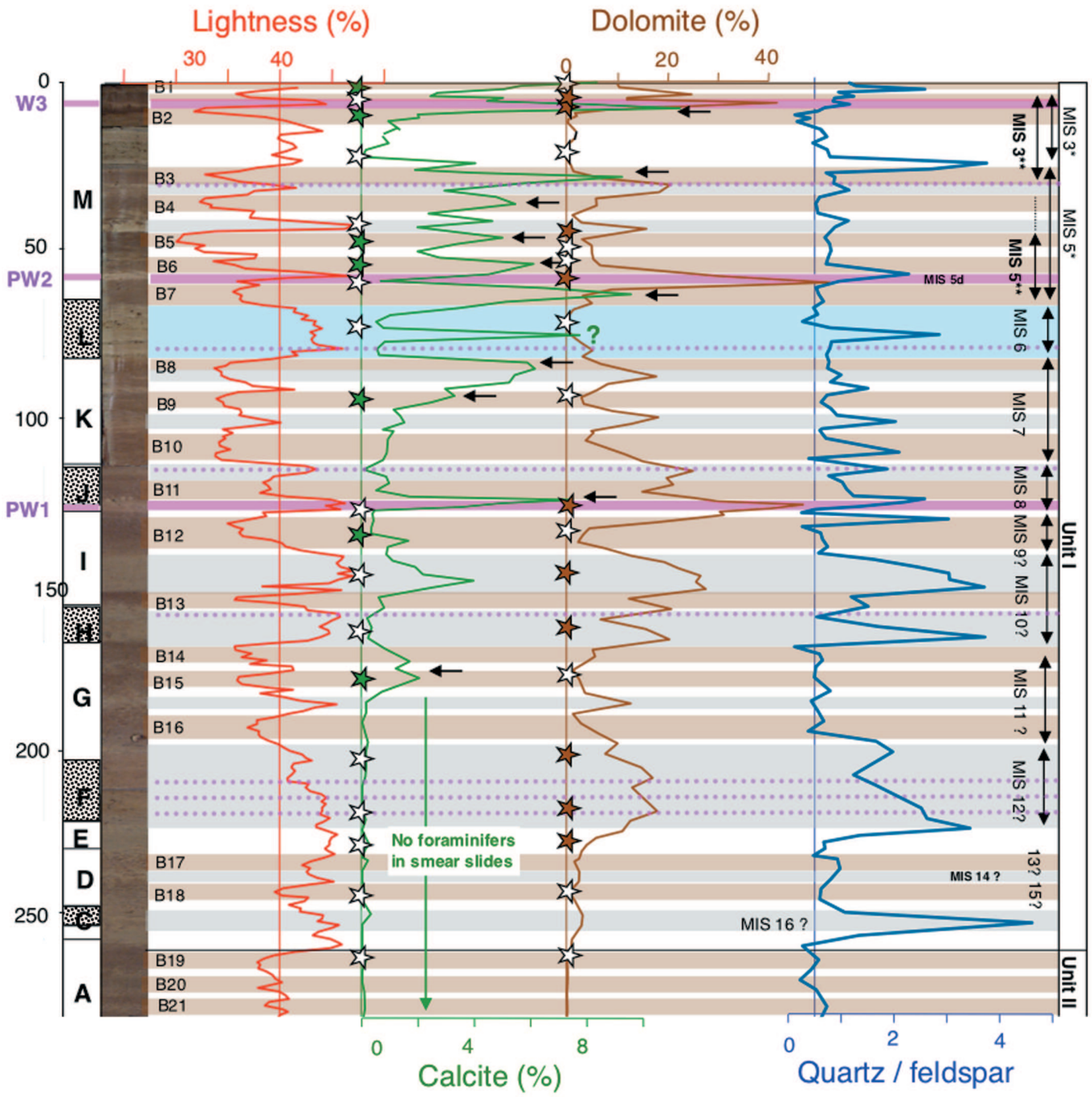

Fig. 8: Lightness L*, calcite (%), dolomite (%), and quartz/feldspar ratios of the upper 280 cm of Core PS72/392-5. Stars indicate depths of studied smear slides (Calcite record: solid/green star = occurrence of foraminifers, open stars = foraminifers absent; dolomite record: solid/brown star = significant occurrence of dolomite, open stars = dolomite absent). In the calcite record, arrows indicate samples where calcite probably has a biogenic origin (i.e., foraminifers and/or coccoliths). At the left hand side, standard lithostratigraphic (SL) units A to M and core photographs showing the dark brown intervals (named as B1 to B21) are shown. At the right-hand side, proposed MIS ages are shown. Proposed MIS stages 3 and 5 based on Polyak et al. (2004, 2009) and ADLER et al. (2009) (*) and BACKMAN et al. (2009) (**), MIS 5d proposed by STEIN (2008). Brownish and dolomite-rich intervals are marked by horizontal brown and gray bars, respectively. MIS 6 is marked as horizontal blue bar. The main pink-white (PW1 and PW2) and white (W3) layers are indicated by pink bars. These layers are characterized by maximum dolomite values. Note that absolute maxima in calcite do not correlate with dolomite maxima and the pink-white layers.

Abb. 8: Helligkeit L* (%; rote Kurve), Kalzit (%; grüne Kurve, Sterne = Vorkommen von Foraminiferen, offene Sterne = keine Foraminiferen), Dolomit (%, braune Kurve, Sterne = signifikante Vorkommen von Dolomit, offene Sterne = kein Dolomit) und Quarz/Feldspat-Verhältnis (blaue Kurve) in den oberen 280 cm von Kern PS72/392-5.

Fig. 7: Sediment core PS72/392-5: Standard lithostratigraphic (SL) units A1 to M, core photographs showing the dark brown intervals (named as 1 to 52 = B1 to B52), lightness L* (%), magnetic susceptibility (10^{-5} SI), wet bulk density (g cm-3), number of IRD grains >2 mm, and content of dolomite (%) of the sequence of core PS72/392-5. More sandy intervals are marked by horizontal light blue bars, probably correlating with periods of maximum ice-sheet extend during glacials MIS 6, MIS 8, MIS 10, MIS 12, and MIS 16. The lower part of SL unit I characterized by maxima in lightness, density and dolomite, probably belongs to MIS 10. The main pink-white (PW1 and PW2) and white (W3) layers are indicated by pink bars. These layers are characterized by maximum dolomite values. At the right-hand side, proposed MIS ages are shown; see also Fig. 8.

Abb. 7: Sedimentkern PS72/392-5: Standard-lithostratigraphische (SL) Einheiten A1 bis M, Kernfotographien mit braunen Lagen B1 bis B52, Helligkeit L* (%, rote Kurve), Magnetische Suszeptibilität (10^{-5} SI, schwarze Kurve), Nassdichte (g cm-3, grüne Kurve), Anzahl von IRD-Partikeln >2 mm (blaue Kurve) und Gehalt an Dolomit (%) ; vgl. auch Abb. 8.

layers at about 26 and 13 cm (37-38 cm and 25-26 cm in GKG core PS72/392-6; see Fig. 5).

Lightness, magnetic susceptibility, density and IRD data

The lightness record of core PS72/392-5 mirrors the dark brown/beige colour cycles in great detail, i.e., the dark-brown to brown intervals coincide with lightness minima (Fig. 7). Besides the short-term cyclicity, there is a long-term change with down-core decreasing lightness values. In general, the more sandy intervals coincide with increased lightness values and minima in magnetic susceptibility. Wet bulk density values, on the other hand, are elevated in the more sandy intervals. With the Unit I/II boundary, the amount of coarse-grained particles >2 mm (interpreted as ice-rafted debris, IRD) significantly increased up-core, more or less contemporaneously with the dolomite content (Fig. 7).

LITHOSTRATIGRAPHY AND AGE MODEL

Lithostratigraphy

As outlined in the introduction, neither untouched archive and fresh sediment material nor standard paleo-records used in modern paleoceanography are available from T3 cores. Thus, one main focus of the geology program of RV "Polarstern" cruise ARK-XXIII/3 was re-coring at one of Clark's key core locations (FL-224; for location see Fig. 1C). This will allow on the one hand to identify and approve Clark's lithostratigraphy and, on the other hand, to use up-to-date tools and methods in paleoceanography needed for a precise core correlation, a development of a more accurate age model, and a more detailed reconstruction of circum-Arctic environmental history.

All the 13 standard lithostratigraphic (SL) units A to M developed by CLARK et al. (1980) could clearly be identified in core PS72/392-5 (Fig. 4; Tab. 2). The more sandy intervals between 249 and 255 cm, 202 and 224 cm, 157 and 168 cm, 114 and 129 cm, and 68 and 83 cm core depth represent SL units C, F, H, J, and L, the uppermost 59 cm represent SL unit M. This classification is further supported by the occurrence of the two most prominent pink-white layers PW1 and PW2 at the base of SL units J and M, respectively, as well as the white layer W3 in the uppermost part of SL unit M (Fig. 4). In Clark's cores, this uppermost part including the layer W3 is often disturbed or even missing. However, undisturbed near-surface sediments were obtained by giant box corer in core PS72/392-6. In this core and in gravity core PS72/392-5, all the key layers PW1, PW2, and W3 are well preserved (Fig. 5). The PW1 layer can even be separated into a lower pink layer and an upper white layer. All three key horizons show the same characteristics in most of the other cores recovered across Mendeleev Ridge during RV "Polarstern" cruise ARK-XXIII/3 and are used – together with the more sandy units – for core correlation (Fig. 5; STEIN et al. 2010, this vol., and 2009b).

In Clark's lithostratigraphy, calcareous foraminifers first occur in SL unit G (Fig. 2). This is supported by the first occurrence of calcite and foraminifers in smear slides in SL unit G of core PS72/392-5 (Fig. 8). The fact that the calcite record is not correlating at all with the detrital dolomite record may suggest that calcite predominantly represents biogenic carbonate. At cores PS72/396-5 and PS72/410-3 (for location see Fig.3), calcareous foraminifers also have their first occurrence in SL unit G (STEIN et al. 2010, this vol.).

The basis of SL unit A was set to 430 cm core depth. Below this depth, the dark brown (to dark reddish brown) colours become more dominant, intercalated by (light) yellowish brown intervals between 455 and 505 cm core depth (Fig. 4; Tab. 2). This lower part of the sedimentary sequence may correlate with Unit A1 described by MUDIE & BLASCO (1985) in the CESAR cores (see also CLARK et al. 1990).

Age model

In this paper, we use the (dark)-brown layers together with specific lithological markers (e.g., pink-white layers, sandy intervals; CLARK et al. 1980) for correlation and for developing an age model of core PS72/392-5 (cf., POLYAK et al. 2004, 2009, DARBY et al. 2006, ADLER et al. 2009, BACKMAN et al. 2009). An alternative – very different – age model mainly based on the assumption that there is a synchronous onset of circum-Arctic diamicton deposition, is discussion by MATTHIESSEN et al. (2010, this vol.).

Basic assumptions of the age model proposed here are (see also STEIN et al. 2010, this vol.):
(1) The (dark) brown intervals coinciding with low lightness values, mainly represent interglacials/interstadials whereas the light/beige intervals are correlated with glacial/stadial intervals (cf., JAKOBSSON et al. 2000, 2001).
(2) The upper seven brown intervals correlate with brown intervals B1 to B7 at cores NP-26 and HLY0503-8JPC (see Fig. 3 for core locations). At these cores, the bases of dark brown intervals B1 and B2 are AMS^{14}C-dated to 11,000 calendar years BP (11 ka) and about 45 ka (POLYAK et al. 2004, 2009). Following these authors, layer W3 should have an age of about 40 ka, and dark brown intervals B4 and B6/7 are correlated with MIS 5a and MIS 5e, respectively. Based on nannofossil stratigraphy of core HLY0503-8JPC, on the other hand, the dark brown layers B5 and B6/7 are correlated with MIS 5a and 5e (BACKMAN et al. 2009). In contrast to BACKMAN et al. (2009) and POLYAK et al. (2009), we propose a MIS 5d age for the pink-white layer PW2 (STEIN 2008, for more details see STEIN et al. 2010, this vol.). At about 30-34 cm, i.e. at the base of brown interval B3, a horizon with very pale brown and pinkish, dolomite-rich clasts occurs, assigned to MIS 5/4 (about 75 ka; age model according to ADLER et al. 2009 and POLYAK et al. 2009) or MIS 4/3 (about 60 ka; age model according to BACKMAN et al. 2009) (Fig. 8).
(3) In core FL-224, the first major down-core polarity change occurred within SL unit K at a core depth of about 100 cm (STEUERWALD et al. 1968, CLARK 1970, CLARK et al. 1980, Fig. 4), now interpreted as geomagnetic excursion and dated to MIS 7 (BACKMAN et al. 2004, POLYAK et al. 2004, SPIELHAGEN et al. 2004, STEIN 2008). This is further supported by nannofossil stratigraphy at core HLY0503-8JPC, suggesting that the dark brown intervals B9 and B10 were deposited during MIS 7 (BACKMAN et al. 2009, see STEIN et al. 2010, this vol. for some more details). Thus, the overlying more sandy part of SL unit L is of MIS 6 age.

(4) Below SL unit K, the age model is still much more tentative (Fig. 7). SL unit J with pink-white layer PW1 at its base is probably of MIS 8 age. This would generally agree with the recently developed age model for Mendeleev Ridge sediments by KAUFMAN et al. (2008). Based on this age model, the PW1 layer corresponds to an age level near the boundary between MIS 8/7 (ADLER et al. 2009, POLYAK et al. 2009). The other more sandy SL units H, F, and C may represent periods of extended ice sheets during the major glacials MIS 10, 12, and 16, respectively (cf., LISIECKI & RAYMO 2005). These sandy (glacial/deglacial) units display maxima in density and minima in magnetic susceptibility (Fig. 7). The prominent density maximum in SL unit I, coinciding with a dolomite maximum and very high quartz/feldspar ratios, is correlated with the upper part of MIS 10 (Fig. 8). For SL unit G characterized by three prominent dark brown intervals and the first occurrence of calcareous foraminifers, an MIS 11 age is proposed.

Using the proposed age model of core PS72/392-5 as well as the brown intervals and pink-white key horizons, it seems to be possible to correlate the PS72/392 record with the record of core PS2185 from Lomonosov Ridge (Fig. 9; SPIELHAGEN et al. 2004; STEIN 2008). In this correlation, the (biogenic) calcite peaks of core PS72/392-5 appear to be more or less contemporaneous with the ^{10}Be and planktic foraminifer peaks determined at core PS2185 and interpreted as interglacials/interstadials (SPIELHAGEN et al. 2004). These findings may support our age model at least for MIS 1 to 8. Certainly, further more detailed studies on core PS72/392-5 sediments are needed to approve this still tentative age model.

Based on the proposed age model, mean sedimentation rates of about 0.5 cm ky^{-1} were calculated for the time interval MIS 1 to 5. Using a mean sedimentation rate of 0.5 cm ky^{-1} for down-core extrapolation, however, the ages of the sandy SL units H, F, and C would be younger than the proposed ages of MIS 10, 12, and 16, respectively. If the latter ages are correct, this would imply that the sedimentation rates below MIS 5 are lower than 0.5 cm ky^{-1}; for more data from other cores and

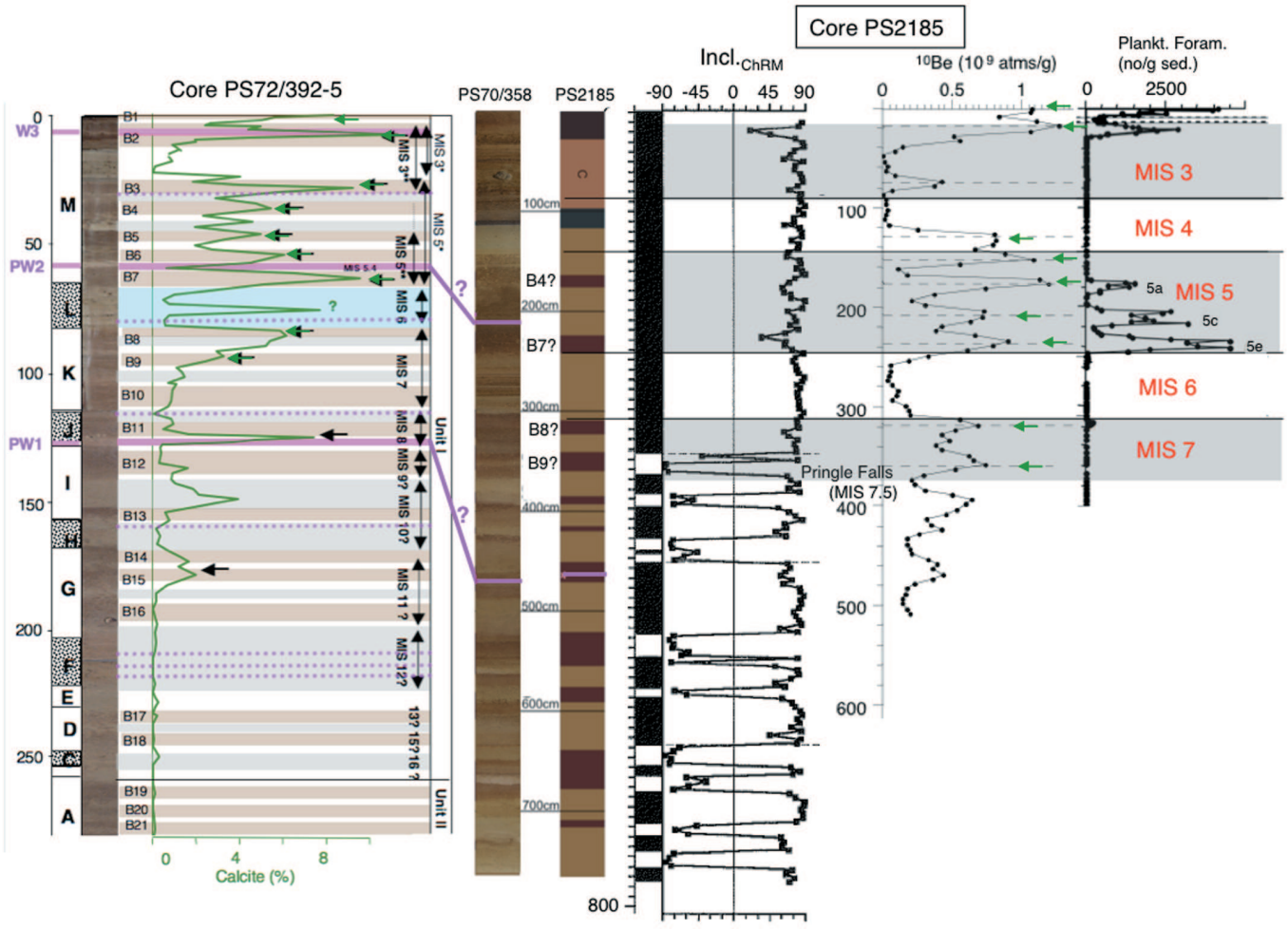

Fig. 9: Standard lithostratigraphic (SL) units A to M, core photographs showing the dark brown intervals (named as B1 to B21), content of (biogenic) calcite (%), and proposed MIS ages of core PS72/392-5, correlated with cores PS2185 and PS70/358 from Lomonosov Ridge. Proposed age model of core PS2185 (MIS 1 to 7) based on SPIELHAGEN et al. (2004); ^{10}Be and planktic foraminifer records from SPIELHAGEN et al. (2004); for details see STEIN (2008). Colour cycles and correlation of cores PS2185 and PS70/358 from STÄRZ (2008), based on FÜTTERER (1992) and Spielhagen in SCHAUER (2008) (for location of cores see Fig. 1C). Intervals with pink-coloured sediments determined at cores PS2185 and PS70/358 by STÄRZ (2008), seem to be correlatable with core PS72/392-5. Proposed MIS stages 3 and 5 based on POLYAK et al. (2004, 2009) and ADLER et al. (2009) (*) and BACKMAN et al. (2009) (**), MIS 5d proposed by STEIN (2008). Most of the (biogenic) calcite maxima at core PS72/392-5 may correlate with 10Be and planktic foraminifer maxima at core PS2185 (green arrows).

Abb. 9: Standard-lithostratigraphische (SL) Einheiten A1 bis M, Kernfotographien mit braunen Lagen B1 bis B21, Gehalt von (biogenem) Kalzit (%) im Sedimentkern PS72/392-5 und Korrelation mit den Kernen PS2185 und PS70/358 vom Lomonosov-Rücken.

discussion see STEIN et al. 2010, this vol.).

ICE-SHEET HISTORY AND PALEOENVIRONMENT: INTERPRETATIONS OF THE PS72/392-5 RECORD

At core PS72/392-5, distinct maxima in IRD >2 mm started to occur at about 255 cm core depth, contemporaneously with the first occurrence of dolomite (Fig. 7). Dolomite is interpreted as indicator for detrital input from the Canadian Archipelago, especially Banks and Victoria Islands, where Paleozoic limestones are cropping out (Fig. 1B; BISCHOF et al. 1996, BISCHOF & DARBY 1997, VOGT 1997, PHILLIPS & GRANTZ 2001). Input from a Canadian source becoming important in the upper part of the sequence (i.e. Unit I), is also supported by the quartz/feldspar and K-feldspar/plagioclase ratios (Fig. 6). Whereas the sediments of Unit II are characterized by dominantly low quartz/feldspar and K-feldspar/plagioclase ratios of <0.7, suggesting the Eurasian shelf seas (i.e., especially the Laptev Sea) as sediment source region, both ratios display distinct peak values of >1 to 4 in Unit I, pointing to the Canadian Archipelago as potential surce region (see VOGT 1997).

These coarse-grained, detrital-carbonate-rich particles were transported by icebergs (and sea ice) via the Beaufort Gyre towards the core location. Thus, these dolomite-rich IRD peaks are related to extended glaciations in the terrestrial North American Arctic at thoses times, i.e., a maximum extension of the Laurentide Ice Sheet (LIS) (Fig. 1B). The disintegration of the ice sheet and ice shelves over the Amerasian Basin may have caused surges and outbursts of icebergs into the Arctic Ocean from the adjacent ice sheets (PHILLIPS & GRANTZ 2001, POLYAK et al. 2004, DARBY et al. 2002, 2006). Such probably short-lived discharge events are reflected in sedimentary records by distinct IRD spikes exemplified by dolomite-rich horizons and – especially – the pink-white layers characterized by peak dolomite contents. At core NP-26 (see Fig. 3 for location), this interpretation is supported by Fe grains indicative of material from the Laurentide part of the Canadian Archipelago and synchronous low oxygen and carbon isotope values of *N. pachyderma,* indicative for meltwater input (POLYAK et al. 2004, DARBY et al. 2006). When did these events of disintegration of the LIS and related IRD pulses occur?

Based on a still preliminary age model, sand-rich intervals are correlated with intervals of an extended ice sheet and its subsequent disintegration during glacials MIS 6, 8, 10, 12, and 16. Except MIS 6, these intervals are characterized by increased dolomite contents, indicating an extended LIS and subsequent disintegration at those times. The two most prominent events reflected in the pink-white layers PW1 and PW2 (CLARK et al. 1980) probably occurred during MIS 8 and MIS 5d (Fig. 8). These events are even recorded on Lomonosov Ridge (Fig. 9). During MIS 6, on the other hand, IRD input from source areas others than Banks/Victoria Islands should have been important. This is in agreement with similar findings in Mendeleev Ridge core NP-26, where MIS 6 is also characterized by the almost absence of detrital carbonate, and Fe oxid composition points to elevated inputs from the Innutian part of the Canadian Archipelago (i.e., Queen Elizabeth Islands) and the Laptev Sea – East Siberian Sea area (POLYAK et al. 2004). Dominantly low quartz/feldspar ratios (Fig. 8) may also be related to a Eurasian source (VOGT 1997, POLYAK et al. 2004). This may even point to the existence of an ice sheet on the East Siberian Shelf (see ADLER et al. 2009, STEIN et al. 2010, this vol.).

Whereas several dolomite peaks coincide with high quartz/feldspar ratios (e.g., during MIS 12, 10, and 8), sometimes the opposite relationship is obvious (e.g., MIS 6 and MIS 3), which may suggest (i) a synchronous and asynchronous evolution of the Laurentide and Eurasian ice sheets, respectively, or (ii) changes in the Transpolar Drift versus Beaufort Gyre circulation systems (STEIN et al. 2010, this vol.). In order to get a more precise identification of source areas and transport pathways of the terrigenous sediment fraction and its interpretation in terms of circum-Arctic glaciations, however, further detailed studies (also including additional sediment cores) are needed.

It is interesting to note that – according to our age model – the onset of coarse-grained dolomite-rich material at core PS72/392-5 (related to IRD input and an extended LIS) probably occurred during MIS 16, the first maximum-sized Quaternary glaciation when looking at the global benthic isotope record (LIESICKI & RAYMO 2005). Exactly at that time, the onset of detrital-carbonate-rich (Heinrich-Event-type) IRD input was also recorded in the North Atlantic at IODP sites U1308 and U1313, interpreted as a signal for the decay of an extended LIS (HODELL et al. 2008, STEIN et al. 2009a, for site location see Figure 1 in STEIN et al. 2010, this vol.). This may suggest that during MIS 16 – for the first time – the LIS was large enough to reach the shelf break and release major amounts of (dolomite-laden) icebergs into the ocean when disintegration started. This still speculative hypothesis, however, has to be approved by further more detailed studies.

CONCLUSIONS

Core PS72/392-5 was recovered during "Polarstern" cruise ARK-XXIII/3 in 2008 in the Nautilus Basin, a small sub-basin of the Canada Basin in the vicinity of the Mendeleev Ridge, at the same location as Clark's key core FL-224. At core PS72/392-5, all the 13 standard lithostratigraphic (SL) units A to M developed by CLARK et al. (1980), including the two most prominent pink-white layers PW1 and PW2 at the base of SL units J and M, respectively, as well as the white layer W3 in the uppermost part of SL unit M, could clearly be identified in core PS72/392-5. Based on our age model, the sand-rich intervals are correlated with glacial maximum/ deglacial phases during the major glacials MIS 6, 8, 10, 12, and 16. Except MIS 6, these intervals are characterized by increased dolomite contents indicating IRD input from the Laurentide Ice Sheet. The dolomite-rich IRD events represented by the PW1 and PW2 layers, are interpreted as short-lived surges and outburts of icebergs during MIS 8 and MIS 5d. For the time interval MIS 1 to 5, mean sedimentation rates of about 0.5 cm ky^{-1} were calculated. Future multi-proxy studies of core PS72/392 and the other cores recovered during RV "Polarstern" cruise 2008 (STEIN et al. 2010, this vol.) as well as similar studies of the new cores recovered during the HOTRAX Expediton 2005 (DARBY et al. 2005, BACKMAN et al. 2009, POLYAK et al. 2009) using up-to-date tools and methods in paleoceanography, will help to solve some of the problems in stratigraphy and chronol-

ogy and will allow more detailed reconstructions of the evolution of the climate history of the Arctic Ocean and its surrounding continents.

ACKNOWLEDGMENTS

We thank captain Stefan Schwarze and his RV "Polarstern" crew for the excellent cooperation during the ARK-XXIII/3 expedition. We also thank the reviewers Robert Spielhagen, Kiel, and Christoph Vogt, Bremen, for numerous constructive suggestions for improvement of the manuscript.
In addition to the authors mentioned,
Evgenia Bazhenova, State University of St. Petersburg, St. Petersburg, Russia,
Sebastian Eckert, Christian März Institute for Chemistry and Biology of the Marine Environment ICBM, Oldenburg University), 26111 Oldenburg,
Alexey Krylov, All-Russian Research Institute for Geology and Mineral Resources VNII OKEANGEOLOGIA St. Petersburg,
Norbert Lensch, Juliane Müller, B. David A. Naafs, Michael Schreck and Isabel Schulte-Loh, Alfred Wegener Institute for Polar and Marine Research AWI, 27568 Bremerhaven,
Seung-il Nam, Korean Institute of Geoscience and Mineral Resources (KIGAM), Yuseong-gu, 305-350 Daejeon, Korea,
Christelle Not, Centre de recherche en Géochimie et en Géodynamique GEOTOP, Université du Québec a Montréal, Montréal, Québec, Canada,
David Poggemann, Leibniz Institute for Marine Sciences IFM-GEOMAR, Kiel University, 24148 Kiel,
participated in the ARK-XXIII/3 Expedition and contributed to the data collected onboard RV "Polarstern" and presented in this paper.

References

Adler, R.E., Polyak, L., Ortiz, J.D., Kaufman, D.S., Channell, J.E.T., Xuan, C., Grottoli, A.G., Sellén, E. & Crawford, K.A. (2009): Sediment record from the western Arctic Ocean with an improved Late Quaternary age resolution: HOTRAX core HLY0503-8JPC, Mendeleev Ridge.- Global Planet. Change 68: 18-29.

Aksu, A.E. & Mudie, P.J. (1985): Magnetostratigraphy and palynology demonstrate at least 4 million years of Arctic sedimentation.- Nature 318: 280-283.

Backman, J., Fornaciari, E. & Rio, D. (2009): Biochronology and paleoceanography of late Pleistocene and Holocene calcareous nannofossil abundances across the Arctic Basin.- Mar. Micropaleont. 72: 86-98.

Backman, J., Jakobsson, M., Løvlie, R., Polyak, L. & Febo, L.A. (2004): Is the central Arctic Ocean a sediment starved basin?- Quat. Sci. Rev. 23: 1435-1454.

Bischof, J.F. & Darby, D.A. (1997): Mid to Late Pleistocene ice drift in the western Arctic Ocean: evidence for a different circulation in the past.- Science 277: 74-78.

Bischof, J., Clark, D. & Vincent, J. (1996): Pleistocene paleoceanography of the central Arctic Ocean: the sources of ice rafted debris and the compressed sedimentary record.- Paleoceanography 11: 743-756.

Clark, D.L. (1970) Magnetic reversals and sedimentation rates in the Arctic Basin.- Geol. Soc. Amer. Bull. 81: 3129-3134.

Clark, D.L., L.A. Chern, L.A., Hogler, J.A., Mennicke, C.M. & Atkins, E.D. (1990): Late Neogene climate evolution of the central Arctic Ocean.- Mar. Geol. 93: 69-94.

Clark, D.L., Whitman, R.R., Morgan, K.A. & Mackey, S.D. (1980): Stratigraphy and glacialmarine sediments of the Amerasian Basin, central Arctic Ocean.- Geol. Soc. Amer. Spec. Pap. 181: 1-57.

Dalrymple, R.W. & Maass, O.C. (1987): Clay mineralogy of late Cenozoic sediments in the CESAR cores, Alpha Ridge, central Arctic Ocean.- Can. J. Earth Sci. 24: 1562-1569.

Darby, D.A. (1975): Kaolinite and other clay minerals in Arctic Ocean sediments.- J. Sed. Petrol. 45: 272-279.

Darby, D.A., Bischof, J.F., Spielhagen, R.F., Marshall, S.A. & Herman, S.W. (2002): Arctic ice export events and their potential impact on global climate during the late Pleistocene.- Paleoceanography 17: doi:10.1029/2001PA000639.

Darby, D.A., Jakobsson, M. & Polyak, L. (2005): Icebreaker expedition collects key Arctic seafloor and ice data.- Eos 86: 549-552.

Darby, D.A. Naidu, A.S., Mowatt, T.C. & Jones, G. (1989): Sediment composition and sedimentary processes in the Arctic Ocean.- In: Y. HERMAN (ed), The Arctic Seas - Climatology, Oceanography, Geology, and Biology, Van Nostrand Reinhold Co., New York, 657-720.

Darby, D.A., Polyak, L. & Bauch, H. (2006): Past glacial and interglacial conditions in the Arctic Ocean and marginal seas - a review.- Prog. Oceanogr. 71: 129-144.

Fütterer, D.K. (1992): ARCTIC'91: The Expedition ARK-VIII/3 of RV "Polarstern" in 1991.- Rep. Pol. Res. 107: 1-267.

Grobe, H. (1987): A simple method for the determination of ice-rafted debris in sediments cores.- Polarforschung 57: 123-126.

Hodell, D.A., Channell, J.E.T., Curtis, J.H., Romero, O.E. & Röhl, U. (2008): Onset of Heinrich Events in the eastern North Atlantic at the end of the Middle Pleistocene Transition (~640 ka)?- Paleoceanography, doi:10.1029/2008PA001591.

Jackson, H.R., Mudie, P.J. & Blasco, S.M. (1985): Initial geological report on CESAR - The Canadian Expedition to study the Alpha Ridge, Arctic Ocean.- Geol. Surv. Can. Pap. 84-22, 1-177.

Jakobsson, M., Backman, J., Murray, A. & Løvlie, R. (2003): Optically stimulated luminescence dating supports central Arctic Ocean cm-scale sedimentation rates.- Geochem. Geophys. Geosyst. 4: 1-11.

Jakobsson, M., Løvlie, R., Al-Hanbali, H., Arnold, E., Backman, J. & Mörth, M. (2000): Manganese and color cycles in Arctic Ocean sediments constrain Pleistocene chronology.- Geology 28: 23-26.

Jakobsson, M., Løvlie, R., Arnold, E.M., Backman, J., Polyak, L., Knutsen, J.-O. & Musatov, E. (2001): Pleistocene stratigraphy and paleoenvironmental variation from Lomonsov Ridge sediments, central Arctic Ocean.- Glob. Planet. Change 31: 1-22.

Jokat, W. (ed) (2009): The Expedition ARK-XXIII/3 of RV Polarstern in 2008.- Rep. Pol. Mar. Res. 597, 221pp.

Kaufman, D.S., Polyak, L., Adler, R., Channell, J.E.T. & Xuan, C. (2008): Dating late Quaternary planktonic foraminifer Neogloboquadrina pachyderma from the Arctic Ocean using amino acids.- Paleoceanography 23: PS3224, doi:10.1029/2008PA001618.

Lisiecki, L.E. & Raymo, M.E. (2005): A Pliocene-Pleistocene stack of 57 globally distributed benthic d18O records. Paleoceanography, 20, PA1003, doi:10.1029/2004PA001071.

Minicucci, D.A. & Clark, D.L. (1983): A Late Cenozoic stratigraphy for glacial-marine sediments of the eastern Alpha Cordillera, central Arctic Ocean.- In: B.F. MOLNIA (ed), Glacial-marine sedimentation. Plenum Press, New York, 331-365.

Moros, M., McManus, J., Rasmussen, T., Kuijpers, A., Dokken, T., Snowball, I., Nielsen, T. & Jansen, E. (2004): Quartz content and the quartz-to-plagioclase ratio determined by X-ray diffraction: a proxy for ice rafting in the northern North Atlantic?- Earth Planet. Sci. Lett. 218: 389-401.

Mudie, P.J. & Blasko, S.M. (1985): Lithostratigraphy of the CESAR cores.- In: H.R. JACKSON, P.J. MUDIE & S.M. BLASKO (eds), Initial Geological report on CESAR: The Canadian Expedition to Study the Alpha Ridge, Geol. Surv. Can. Pap. 84-22, 59-99.

Nørgaard-Pedersen, N., Mikkelsen, N., Lassen, S.J. & Kristoffersen, Y. (2007): Arctic Ocean record of last two glacial-interglacial cycles off North Greenland/Ellesmere Island - Implications for glacial history.- Mar. Geol. 244: 93-108.

Nowaczyk, N.R., Antonow, M., Knies, J. & Spielhagen, R.F. (2003): Further rock magnetic and chronostratigraphic results on reversal excursions during the last 50 ka as derived from northern high latitudes and discrepancies in precise AMS14C dating.- Geophys. J. Internat. 155: 1065-1080.

Nowaczyk, N.R., Frederichs, T.W., Kassens, H., Norgaard-Pedersen, N., Spielhagen, R., Stein, R. & Weiel, D. (2001): Sedimentation rates in the Makarov Basin, central Arctic Ocean: a paleomagnetic and rock magnetic approach. Paleoceanography 16, 368-389.

Petschick, R. (2000): MacDiff 4.2. Manual, http://www.geologie.uni-frankfurt.de/staff/Homepages/Petschick/PDFs/MacDiff_Manual_D.

Phillips, R.L. & Grantz, A. (2001): Regional variations in provenance and abundance of ice-rafted clasts in Arctic Ocean sediments: Implications for the configuration of Late Quaternary oceanic and atmospheric circulation in the Arctic.- Mar. Geol. 172: 91-115.

Polyak, L., Bischof, J., Ortiz, J.D., Darby, D.A., Channell, J.E.T., Xuan, C., Kaufman, D.S., Løvlie, R., Schneider, D.A., Eberl, D.D., Adler, R. & Council, E.A. (2009): Late Quaternary stratigraphy and sedimentpattern in the western Arctic Ocean. Glob. Plan. Change, in press.

Polyak, L.V., Curry, W.B., Darby, D.A., Bischof, J. & Cronin, T.M. (2004): Contrasting glacial/interglacial regimes in the western Arctic Ocean as exemplied by a sedimentary record from the Mendeleev Ridge.- Palaeogeogr. Palaeoclim. Palaeoecol. 203: 73-93.

Schauer, U. (ed) (2008): The expedition ARK/XXII-2 of the Research Vessel "Polarstern" in 2007 - a contribution to the International Polar Year 2007/08.- Rep. Pol. Mar. Res. 579, 279 pp.

Sellén, E., Jakobsson, M. & Backman, J. (2008): Sedimentary regimes in Arctic's Amerasian and Eurasian Basins: clues to differences in sedimentation rates.- Global Planet. Change 61: 275-284.

Spielhagen, R.F, Baumann, K.-H., Erlenkeuser, H., Nowaczyk, N.R., Nørgaard-Pedersen, N., Vogt, C. & Weiel, D. (2004): Arctic Ocean deep-sea record of Northern Eurasian ice sheet history.- Quat. Sci. Rev. 23: 1455-1483.

Stärz, M. (2008): Stratigraphie und Paläoumwelt im Arktischen Ozean während des mittleren Pleistozäns: Rekonstruktion aus Sedimentabfolgen vom Lomonosov-Rücken.- Unpubl. Bachelor Thesis, Univ. Freiberg.

Stein, R. (2008): Arctic Ocean Sediments: Processes, Proxies, and Palaeoenvironment. Elsevier, Amsterdam, Developments in Marine Geology, 2: 1-587.

Stein, R., Hefter, J., Grützner, J., Voelker, A. & Naafs, D. (2009a): Variability of surface-water characteteristics and Heinrich Events in the Pleistocene mid-latitude North Atlantic Ocean: Biomarker and XRD records from IODP Site U1313 (MIS 16-9).- Paleoceanography 24, PA2203, doi:10.1029/2008PA001639

Stein, R., Krylov, A., Matthiessen, J., Nam, S., Niessen, F. & the ARK-XXIII/3 Geology Group (2009b): Main lithologies and lithostratigraphy of ARK-XXIII/3 sediment cores.- In: W. JOKAT (ed), The Expedition ARK-XXIII/3 of RV Polarstern in 2008,- Rep. Pol. Mar. Res. 597: 12-86.

Stein, R., Matthiessen, J., Niessen, F, Krylov, A., Nam, S.-il, & Bazhenova, E. (2010): Towards a better (litho-)stratigraphy and reconstruction of Quaternary paleoenvironment in the Amerasian Basin (Arctic Ocean).- Polarforschung 79(2): 97-121.

Steuerwald, B.A., Clark, D.L. & Andrew, J.A. (1968): Magnetic stratigraphy and faunal patterns in Arctic Ocean sediments.- Earth Planet. Sci. Lett. 5: 79-85.

Vogt, C. (1997): Regional and temporal variations of mineral assemblages in Arctic Ocean sediments as climatic indicator during glacial/interglacial changes. Reps. Pol. Res. 251, 309 pp.

Vogt, C. (2009): Data report: semiquantitative determination of detrital input to ACEX sites based on bulk sample X-ray diffraction data.- In: J. Backman, K. Moran, D.B. McInroy, L.A. Mayer & the Expedition 302 Scientists, Proc. IODP, 302: Edinburgh, Integrated Ocean Drilling Program Management Internat. Inc. doi:10.2204/iodp.proc.302.203.2009 12 pp.

Weber, M.E., Niessen, F, Kuhn, G. & Wiedicke, M. (1997): Calibration and application of marine sedimentary physical properties using a multi-sensor core logger. Mar. Geol. 136, 151-172.